Accepted Manuscript

Optimal Planning of the Joint Placement of Photovoltaic Panels and Green Roofs Under Climate Change Uncertainty

Mohammad Ramshani, Anahita Khojandi, Xueping Li, Olufemi Omitaomu

PII: \$0305-0483(17)31151-9

DOI: https://doi.org/10.1016/j.omega.2018.10.016

Reference: OME 1986

To appear in: Omega

Received date: 22 November 2017
Revised date: 5 October 2018
Accepted date: 23 October 2018



Please cite this article as: Mohammad Ramshani, Anahita Khojandi, Xueping Li, Olufemi Omitaomu, Optimal Planning of the Joint Placement of Photovoltaic Panels and Green Roofs Under Climate Change Uncertainty, *Omega* (2018), doi: https://doi.org/10.1016/j.omega.2018.10.016

This is a PDF file of an unedited manuscript that has been accepted for publication. As a service to our customers we are providing this early version of the manuscript. The manuscript will undergo copyediting, typesetting, and review of the resulting proof before it is published in its final form. Please note that during the production process errors may be discovered which could affect the content, and all legal disclaimers that apply to the journal pertain.

Highlights

- We propose an approach to investigate the joint placement of Photovoltaic (PV) panels, the fastest growing renewable technology, and green roofs, a sustainable solution for energy saving, to improve the output efficiency of PV panels.
- We develop a two-stage stochastic programming model to incorporate PV panel/green roof placement decisions under different, at times conflicting, climate models to maximize the overall profit from energy generated and saved.
- We calibrate the models using historical data, industry reports, future projections of temperature and precipitation, as well as expert opinion to examine a real-world case study and provide insights.
- Due to the large solution space of the case study, we used a Benders' decomposition (L-shaped method) to obtain the solution within a tractable time frame.
- The results show that the joint placement of PV panels and green roofs contributes to a higher profit through additional energy generated.
- The results suggest that the PV-GR integration efficiency increase is an important contributing factor in the placement decisions, hence highlighting the need for further investigation in characterizing this factor in future studies.
- The results suggest that the model is sensitive with respect to green roof-related parameters, suggesting the need for careful calibration of these parameters before large scale implementation in any climate region.
- The results indicate that considering the long-term changes in the rate of energy consumption affects the distribution of budget/rooftop areas between PV panels and green roofs.

Optimal Planning of the Joint Placement of Photovoltaic Panels and Green Roofs Under Climate Change Uncertainty

Mohammad Ramshani^a, Anahita Khojandi^{a,*}, Xueping Li^a, Olufemi Omitaomu^{a,b}

^aDepartment of Industrial and Systems Engineering, The University of Tennessee at Knoxville, Knoxville, TN 37996, US

^b Urban Dynamics Institute, Oak Ridge National Laboratory, Oak Ridge, Tennessee 37831, US

Abstract

Photovoltaic (PV) panels directly convert sunlight into electricity; but, sunlight also heats the panels, negatively impacting their efficiency. Green roofs are vegetative layers grown on rooftops, mainly to provide added insulation on the roof to save energy. Green roofs also cool near-surface air temperature. Hence, the joint installation of PV panels and green roofs may potentially lead to higher efficiency of PV panels in certain climates. We develop a two-stage stochastic programming model to optimally place PV panels and green roofs under climate change uncertainty to maximize the overall profit from energy generated and saved. We calibrate the model using the literature, industry reports, and the data from different, at times conflicting, climate projections. We then conduct a case study for a mid-size city in the U.S., perform extensive sensitivity and robustness analyses and provide insights. Keywords: Stochastic optimization, renewable energy generation, energy savings, climate change

1. Introduction

Greenhouse gases are the most important contributing factor to the increase of average global temperatures over time (Bose, 2010); at the current pace, it is estimated that the

Email address: khojandi@utk.edu (Anahita Khojandi)

^{*}Corresponding author

global temperature will rise by up to 5.8 degrees Celsius over the next century (Rehman et al., 2007). Greenhouse gas emissions are primarily caused by burning fossil fuels (Schneising et al., 2014) and without a significant change in energy production policies, specifically to reduce the reliance on fossil fuels, the current concentrations of greenhouse gases in the atmosphere is only expected to grow (Hoffert et al., 1998).

Solar power is a clean, free, and promising renewable energy source that helps reduce greenhouse gas emissions and hence, mitigate global warming and climate change. Photovoltaic (PV) panels, which can directly convert sunlight into electricity, are one of the most efficient methods of harnessing solar power. PV panels are the fastest growing renewable technology in the recent years at an annual average rate of 6.8% (EIA, 2015). The number of panels installed within the U.S. increased by 63% between 2007 and 2008 (Scherba et al., 2011), with an estimated increase of approximately 30% per year from 2013 through 2016 in the residential sector (EIA, 2015). This rate of growth can be attributed to the decreasing costs of PV panels (Feldman et al., 2014) as well as the incentives provided by state and federal governments. The falling prices of PV panels, coupled with the overall increases in power costs from conventional sources, suggest that PV panels are on track to become a strategically advantageous solution to sustainable energy production (Yang, 2010). It is, however, important to note that despite the increase in demand and the popularity of PV panels, efficiency of PV panels is still limited and depend mainly on the panels' cell material and their operating temperature. The open circuit voltage shows a drop of 2.3 mV per 1 degree Celsius rise in temperature, which translates to a 0.5% drop in efficiency per degree Celsius rise in temperature (Witmer, 2010). While there is ongoing research into engineering solutions to increase the efficiency of PV panels, this paper explores an immediate operational solution through improved, systemic placement decisions.

According to the U.S. Energy Information Administration (EIA), 47.7% of the energy consumed by residential households and 34% of the energy used by the commercial sector is due to space conditioning (i.e., heating and cooling) (EIA, 2015). Given an expected average growth rate of 0.4%–1.2% and 0.9%–1.1% in the residential and commercial sectors, respectively, it is estimated that by 2040 the number of residential households grows to 150



Figure 1: GR integrated PV panel installed over a rooftop in Hailey, Idaho (SVS, 2017).

million and the commercial space increases to 110 billion square feet (EIA, 2015). Hence, any reduction in the energy required for space conditioning can result in substantial cost/energy savings. Green roofs (GRs), which are vegetative layers grown on rooftops, can provide added insulation on the roof and cool near-surface air temperature through decreasing the absorption rate of solar radiation by the building structure (Dunec, 2012). This cooling effect can contribute to an approximately 30% drop in the surface temperature (Dunec, 2012). Several long-term studies are currently underway to quantify the thermal performance of GRs (Niachou et al., 2001; Sonne, 2006) as well as the relationship between GRs and energy savings (Coma et al., 2016; Refahi and Talkhabi, 2015) under different climatic conditions. So far, it is estimated that widespread installation of GRs throughout the U.S. can result in \$7-\$10 billion in savings (Dunec, 2012).

In addition to direct savings in space conditioning costs, GRs can contribute to energy production of PV panels if they are jointly installed. Specifically, GRs create a cool microclimate in hot weather and reduce the temperature of their surrounding area. Hence, their joint installation with PV panels (Figure 1) can help cool down the panels, allowing them to function at a higher efficiency. The increase in panel efficiency is consistently reported in the literature; however, the degree of this increase varies from one study to another, ranging between 0.08% and 8.3% across studies of various lengths, conducted in different

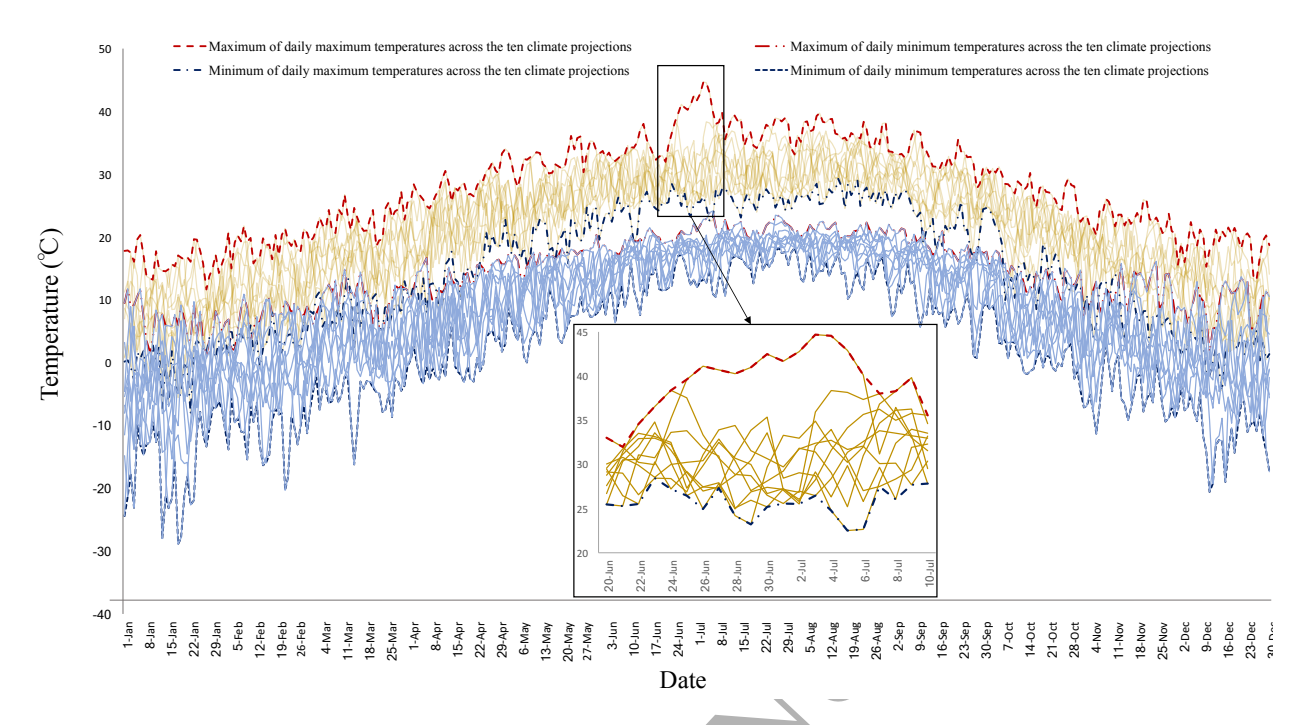


Figure 2: The daily maximum and minimum temperatures for the City of Knoxville, Tennessee from ten different climate projections for the year 2030. The dashed lines present the maximum and minimum temperatures across the ten projections over the year. (For details on the climate projections refer to Table 3.)

climates (Chemisana and Lamnatou, 2014; Hui and Chan, 2011; Köhler et al., 2007; Witmer and Brownson, 2011).

The degree of benefit from PV panels and GRs highly depends on the weather and climate conditions of the location in which they are installed (Refahi and Talkhabi, 2015; Witmer, 2010). However, the information on how the weather and/or climate conditions evolve over time in specific regions/locations are limited and often unreliable. Indeed, although the global trend of climate change is consistently reported, in general there is no consensus among current climate projections and their evolution over time in specific regions/locations (Jun et al., 2008). For instance, Figure 2 presents the daily maximum and minimum temperatures for the City of Knoxville, Tennessee from ten different climate projections for the year 2030, provided by Oak Ridge National Laboratory's Urban Dynamics Institute (UDI) (UDI, 2017) and Oak Ridge National Laboratory's Climate Change Science Institute (CCSI) (CCSI, 2017). As seen in the figure, the projections can differ by up to approximately 25.4 and 37.1 degrees Celsius for daily maximum and minimum temperatures, respectively, in a given

day. Hence, using each of these forecasts to guide future benefits of installing PV panels and GRs, either separately or jointly, may result in a different set of recommendations.

PV panels and GRs are relatively expensive and have long lifespans, and hence, they are both considered long-term investments. PV panels can generally retain a high efficiency of 80%-85% up to 20 years after installment (Energy Informative, 2017). Similarly, GRs are reported to last on the order of 40 years (Porsche and Köhler, 2013; Minnesota Stormwater Manual, 2018), almost twice as long as traditional roofs. Therefore, it is important to carefully plan such investments to maximize their expected return.

In this paper, we present an approach to consolidate a set of future climate projections when making long-term investment decisions on the installation of PV panels and GRs, from the perspective of a regional governing body. Specifically, we develop a two-stage stochastic programming model to determine the optimal placement of PV panels and GRs, either separately or jointly, among a set of candidate rooftops. Our objective is to maximize the profit from the energy generated and saved using these practices, considering the uncertainties in the future evolution of the climate and the positive interaction of PV panels and GRs in increasing PV panels' efficiency. We develop a profit-maximizing model to allow governing bodies and policy makers to carefully evaluate their options before making an investment.

Optimal placement problems are studied in a wide array of domains and applications (e.g., for the placement of distributed generation source (Wang and Nehrir, 2004), phasor measurement units (Gou, 2008), multiple allocation hubs (Correia et al., 2018), and wind turbines (Marmidis et al., 2008), or in facility location problems (Albareda-Sambola et al., 2011)). In this paper, we formulate an optimal placement problem for joint installation of PV panels and GRs. In the literature, studies involving PV panels mostly focus on underlying PV material or cell technology (Tyagi et al., 2013; Chow, 2010; Kasper et al., 2014). Alternatively, there is a body of work that aims to determine the best placement option for individual PV panels. For instance, there are a number of studies that evaluate rooftop characteristics to calculate individual rooftop solar access using geographic information system (GIS) (Levinson et al., 2009; Wiese et al., 2010; Van Hoesen and Letendre, 2010; Ordóñez et al., 2010), or aim to develop GIS-based models to optimize electricity generation

estimation of PV panels installed on rooftops (Hong et al., 2014).

95

115

Additionally, there exist studies whose objectives are to find the optimal installation criteria for PV panels, e.g., size, tilt angle, converter properties. An integrated multiobjective optimization model is developed in (Koo et al., 2016) to determine rooftop-specific
installation criteria for PV panels to maximize their energy production effectiveness and
efficiency. Similarly, a particle swarm optimization algorithm is developed in (Kornelakis,
2010) to find the optimal installation details (i.e., number of PV modules, their optimal
tilt angle and distribution among the DC-AC converters) for a grid-connected PV system to
maximize the total net profit and environmental benefits of the system. In another study (Liu
et al., 2012), a simulation model is developed to find the optimal size and slope of PV systems
under certain climate conditions subject to equipment costs as well as electricity and saleback tariffs. In a similar vein, in (Chen, 2013), a Bayesian approach is used to optimally
size stand-alone PV systems under climate change uncertainty.

There exist only a few large scale studies that attempt to optimize the implementation of PV panels. In (Arnette, 2013), the output of large scale renewable energy farms (both wind and solar) is evaluated and compared with that of rooftop PV panels, after minimizing energy generation costs and greenhouse gas emissions. In another study (Park et al., 2016), the optimal strategy to implement PV systems to achieve national carbon emission reduction targets is proposed. None of these large scale studies, however, consider future climate scenarios to capture the uncertainty in output of PV panels, nor do they take into account GRs, their energy saving properties, or their interactions with PV panels.

The literature related to GRs mainly focuses on their many potential environmental benefits, e.g., management of runoff water quality and quantity (Berndtsson, 2010), reduction of heat island and improvement of urban comfort (Santamouris, 2014), contribution to plant and ecological diversity (Cook-Patton and Bauerle, 2012), and reduction of urban air pollution (Yang et al., 2008), to name a few. Also, a major group of studies explore GRs' physical properties, e.g., types of substrate (Ampim et al., 2010), hydrologic performance (Li and Babcock, 2014), thermal behavior (Niachou et al., 2001), and vegetation types (Snodgrass and Snodgrass, 2006).

There exits a few studies in the literature that attempt to optimize energy savings/cost reductions achieved using GRs. For instance, Gargari et al. (2016) simulate the thermal behavior of a building covered with GRs in order to optimize the energy savings achieved by installing green media on the rooftop of a building. The results show that the installation of GRs for buildings that meet the most recent insulation regulations leads to moderate levels of energy savings. In another study, Kim et al. (2012) investigate the economic and environmental benefits of GRs through an optimal-scenario selection model. The authors preform life-cycle cost analysis for fifteen different types of GRs and conclude that the cost reductions and environmental benefits achieved by GRs are noteworthy. Chang et al. (2010) conduct a cost-benefit optimization on GR sizes. Their results show that the amount of energy savings increases in the size of GR. Despite their contributions, none of these studies, however, examine the optimal placement of GRs in a large scale study.

Stochastic programming has been extensively used in the literature for modeling long-term planning problems under uncertainty (Birge and Louveaux, 2011). Specifically, two-stage stochastic programming has been widely applied in a variety of studies including but not limited to portfolio selection (Abdelaziz et al., 2007), transportation planning (Barbarosolu and Arda, 2004), disaster management (Noyan, 2012), waste management (Maqsood and Huang, 2003), scheduling (Parisio and Jones, 2015), and distributed energy systems (Zhou et al., 2013). Similar to other works in the literature, here we aim to incorporate uncertainty about the future through a set of possible scenarios. However, to the best of our knowledge, this is the first study that uses such approach for incorporating climate change into urban planning over a long planning horizon.

135

145

Various cities or states in the U.S. have invested in, or are currently leading, projects to place green infrastructure and/or energy-efficient practices and technologies EPA (2009); The City of Knoxville (2018); EPA (2017). Most of these projects, however, are focused on investing in a single geographic region or a small community, and involve a single type of practice alone (e.g., solar panels, LED lights, green infrastructure). In this study, we take a forward-looking view and provide a general model that can account for joint placement of GRs and PV panels across various geographical regions simultaneously. To the best of our

knowledge, this is the first model that accounts for multi-region, multi-practice placement, hence allowing policy makers to plan large-scale implementations, while accounting for the potential interactions between the practices.

The remainder of this paper is organized as follows. First we clearly define the scope of the problem and present the model formulation in Section 2. Next, in Section 3, we calibrate the model using the literature, industry reports and a few datasets. In Section 4, we first discuss the solution approach. Next we conduct a case study for a mid-sized city in the U.S., namely, Knoxville, Tennessee, perform sensitivity and robustness analyses, and provide environmental insights. Lastly, we conclude in Section 5.

2. Model Formulation

155

165

175

In this section, we present a two-stage stochastic programming model with complete recourse to determine the placement of PV panels and GRs to maximize the overall profit. The first stage decisions are to choose a set of candidate sites to install PV panels and GRs, either separately or jointly. After all uncertainties are realized, second stage decisions, i.e., the amount of electricity sold to or purchased from the grid, are made. Note that consistent with the current practice, we assume that excess energy generated by PV panels can be sold to the grid (Banos et al., 2011). In the remainder of the paper, the word *energy* refers to electrical energy unless otherwise stated.

Let T denote the planning horizon and K denote the set of regions, where I^{κ} denotes the set of candidate sites within region $\kappa \in K$. Let the discrete random variable W with probability mass function p_W denote the sample path of the future climate evolution for the regions of interest over the planning horizon. Let η_{ω} denote the realization probability of scenario $\omega \in \Omega$, where Ω is a finite discrete set of projected climate scenarios, i.e., $\eta_{\omega} = p_W(\omega)$.

Let the first stage binary variables x_i^{κ} and y_i^{κ} denote whether or not PV panels and GR are installed at candidate site $i \in I^{\kappa}$, respectively, where each assumes the value 1 if the corresponding practice is installed at site $i \in I^{\kappa}$ and equals to 0, otherwise. Let k_i^{κ} denote the total area of PV panel installed at site $i \in I^{\kappa}$. Let c_i^{κ} and g_i^{κ} denote the cost of installing PV system and GR at site $i \in I^{\kappa}$, respectively.

Sets	
Ω	Set of climate scenarios, where $\omega \in \Omega$
K	Set of regions, where $\kappa \in K$
I^{κ}	Set of candidate sites in region $\kappa \in K$, where $i \in I^{\kappa}$
First Stage Variables	bet of candidate blees in region to C 11, where t C 1
x_i^{κ}	Equals 1 if PV panels are installed at site i in region κ and 0, otherwise
y_i^{κ}	Equals 1 if GR is installed at site i in region κ and 0, otherwise
c_i^{κ}	Installation cost of PV system at site i in region κ (USD)
g_i^{κ}	Installation cost of GR at site i in region κ (USD)
k_i^{κ}	Area of PV panel installed at site i in region κ (m ²)
Second Stage Variables	
$e^{\kappa}_{i\omega}$	Energy generated by PV panels at site i in region k under scenario ω (kWh)
$s_{i\omega}^{\kappa}$	Energy saved by GR at site i in region κ under scenario ω (kWh)
r_{ω}^{κ}	Energy sold to the grid in region κ under scenario ω (kWh)
ϕ_{ω}^{κ}	Energy purchased from the grid in region κ under scenario ω (kWh)
Parameters	
F	PV system fixed cost (USD)
Q	PV panel output (W)
B	Initial budget available for investment (USD)
γ	Cost per kWh purchased from the grid (USD)
μ	Price per kWh sold to the grid (USD)
α	Percentage energy saving in cooling degree-hours due to GR installation
β	Percentage energy saving in heating degree-hours due to GR installation
heta	Percentage efficiency increase in the output of PV panels due to integration with GRs
δ	Percentage change in energy consumed for space conditioning over the planning horizon
V^{κ}	PV system variable cost in region κ (USD)
\mathbb{C}^{κ}	Total maintenance cost per m ² PV panel installed in region κ (USD)
P^{κ}	Cost per m^2 for installing GR in region κ (USD)
R^{κ}	Total energy requirement for space conditioning in region κ over the planning horizon (kWh)
η_ω	The realization probability of scenario ω , where $\sum_{\alpha} \omega \eta_{\omega} = 1$
A_i^{κ}	Rooftop surface available at site i in region κ (m ²)
H_i^{κ}	Average hourly electricity consumption for space conditioning at site i in region κ (kWh)
ι_i^{κ}	Rooftop radiation potential of site i in region κ
Stochastic Parameters	
L^{κ}_{ω}	Total number of peak sunlight hours available in region κ under scenario ω over the planning horizon
λ_ω^κ	Total number of cooling degree-hours in region κ under scenario ω over the planning horizon
$ au_\omega^{\widetilde{\kappa}}$	Total number of heating degree-hours in region κ under scenario ω over the planning horizon

Table 1: Notation used in the model.

Let the second stage variables $e_{i\omega}^{\kappa}$ and $s_{i\omega}^{\kappa}$ denote the amount of energy generated and saved in kWh at candidate site $i \in I^{\kappa}$ under scenario $\omega \in \Omega$, respectively. Additionally, let H_i^{κ} denote the average hourly electricity consumption at each candidate site $i \in I^{\kappa}$ to maintain the building temperature via air conditioning, and R^{κ} denote the total required electricity for space conditioning in region $\kappa \in K$ over the planning horizon. Let δ denote the percentage change in energy consumed for space conditioning over the planning horizon, due to an array of technological, sociological, climatic, and economic factors. Lastly, let B denote the initial budget available for investment.

180

PV panels rely on solar irradiation to generate electricity and their outputs significantly differ depending on the number of hours they are exposed to sunlight. A 'peak sunlight hour' is typically used to describe the intensity of sunlight in a specific area, where 1 peak sunlight hour is equivalent to 1 kWh/m² (Aurora Energy, 2018; Solar Power Authority, 2018). Hence, the number of peak sunlight hours for a day represents the accumulative solar irradiation over the course of the day. Additionally, the level of solar radiation received by any rooftop depends on a variety of factors, e.g., aspect of the building, rooftop slope, and the shadowing effect or solar access to buildings. Let ι_i^{κ} denote the rooftop solar radiation potential at site $i \in I^{\kappa}$, which quantifies the percentage of daily available sunlight that an average rooftop at site $i \in I^{\kappa}$ receives. Let the stochastic parameter L_{ω}^{κ} denote the total number of peak sunlight hours available over the planning horizon in region $\kappa \in K$ under scenario $\omega \in \Omega$.

Cooling and heating degree-hours are measures of how many degrees and for how long the outside temperature is above or below certain base temperatures, respectively (Degree Days Weather Data, 2017). These metrics are typically used to determine whether or not space heating and cooling are required for buildings. Let $\lambda_{\omega}^{\kappa}$ and τ_{ω}^{κ} denote the total number of cooling and heating degree-hours over the planning horizon, during which space cooling and heating are required, respectively, for buildings in region $\kappa \in K$ under scenario $\omega \in \Omega$. Additionally, let α and β denote the percentage of energy saving due to GR installation in cooling and heating degree-hours, respectively. Lastly, recall that the joint installation of PV panels and GRs positively affect the PV panels output. Let θ denote the percentage increase in the output of PV panels as a result of their integration with GRs. Table 1 summarizes

all the notation used in model formulation.

Recall that our objective is to maximize the profit from energy generated and saved, i.e.,

$$Z = \max \sum_{i} \sum_{\kappa} -(Fx_i^{\kappa} + k_i^{\kappa}V^{\kappa} + A_i^{\kappa}P^{\kappa}y_i^{\kappa}) + \sum_{\omega} \sum_{\kappa} \eta_{\omega}(r_{\omega}^{\kappa}\mu - \phi_{\omega}^{\kappa}\gamma). \tag{1}$$

The first term inside the maximization corresponds to the installation cost of PV panels and GRs in a subset of candidate sites across all regions. The second term inside the maximization corresponds to energy generated and saved under all scenarios across all regions. The following equations, i.e., Equations (2) - (9), present the constraints of the model,

$$g_i^{\kappa} = A_i^{\kappa} P^{\kappa} y_i^{\kappa} \qquad \forall i, \kappa, \tag{2}$$

$$c_i^{\kappa} = F x_i^{\kappa} + k_i^{\kappa} (V^{\kappa} + \mathbb{C}^{\kappa}) \qquad \forall i, \kappa,$$
(3)

$$\sum_{i} \sum_{\kappa} (e_i^{\kappa} + g_i^{\kappa}) \le B,\tag{4}$$

$$k_i^{\kappa} \le A_i^{\kappa} x_i^{\kappa} \qquad \forall i, \kappa, \tag{5}$$

$$e_{i\omega}^{\kappa} = Q L_{\omega}^{\kappa} k_{i}^{\kappa} \iota_{i}^{\kappa} (1 + y_{i}^{\kappa} \theta) \qquad \forall i, \omega, \kappa,$$

$$(6)$$

$$s_{i\omega}^{\kappa} = H_i^{\kappa} y_i^{\kappa} (\alpha \lambda_{\omega}^{\kappa} + \beta \tau_{\omega}^{\kappa}) \qquad \forall i, \omega, \kappa,$$
 (7)

$$\sum_{i} (e_{i\omega}^{\kappa} + s_{i\omega}^{\kappa}) + \phi_{\omega}^{\kappa} - r_{\omega}^{\kappa} \ge (1 + \delta)R^{\kappa} \qquad \forall \omega, \kappa,$$
(8)

$$r_{\omega}^{\kappa} \le \sum_{i} e_{i\omega}^{\kappa} \qquad \forall \, \kappa, \omega.$$
 (9)

Consistent with the literature (Coma et al., 2016; Refahi and Talkhabi, 2015; Dunec, 2012), we assume that if the decision is to install GR at site $i \in I^{\kappa}$, it must be large enough to completely cover the rooftop; hence, Equation (2) calculates the GR installation cost at site i in region κ . Equation (3) links the PV system cost, c_i^{κ} , to its two different components, namely, PV system fixed cost, denoted by F, and PV system variable and maintenance costs in region κ , denoted by V^{κ} and \mathbb{C}^{κ} , respectively. Note that PV panels require very little maintenance (Boston Solar, 2018; Whaley, 2016), while extensive GRs are essentially cost-saving compared with conventional roofs when it comes to maintenance (GSA, 2011; Green Infrastructure Foundation, 2017; Wong et al., 2011). In this study, we assume the property owner is responsible for maintenance costs, whether or not their properties are selected by the model as candidates for placement of the green practices, i.e., $\mathbb{C}^{\kappa} = 0$. We revisit this assumption in our computational study in Section 4.3 to investigate the impact of incorporating maintenance costs directly into the model.

Equation (4) limits the total cost of PV systems and GRs to a given budget B. Equation (5) guarantees that the area covered with PV panels cannot exceed the available rooftop surface. Note that simultaneous installation of PV panels and GRs on a rooftop is possible as PV panels are generally installed slightly elevated above the roof surface.

Recall that the integration of PV panels and GRs can help cool down the panels, thereby resulting in a higher electricity output. Therefore, Equation (6) calculates the energy generated by PV panels at site $i \in I^{\kappa}$ under scenario $\omega \in \Omega$.

230

The amount of energy savings from GR at each candidate site is given by Equation (7). The amount of electricity sold to or purchased from the grid, r_{ω}^{κ} and ϕ_{ω}^{κ} , respectively, serve as second stage decisions in the model. We assume that each region has certain energy requirements for space conditioning over the planning horizon. Hence, Equation (8) guarantees that for each region the total energy generated, $e_{i\omega}^{\kappa}$, and saved, $s_{i\omega}^{\kappa}$, and the total electricity sold to the grid, r_{ω}^{κ} , or purchased from the grid, ϕ_{ω}^{κ} , is at least equal to the energy requirement for space conditioning of the region. Lastly, Equation (9) assures that the electricity sold to the grid cannot exceed the electricity generated by systems.

Note that the placement problem (1)-(9) has complete recourse. That is, for all the first-

stage decisions, regardless of the uncertainties, there exists at least one feasible second-stage decision (Birge and Louveaux, 2011).

3. Model Calibration

245

In this section, we use the literature and a series of datasets to calibrate the model formulated in Section 2 to further conduct a case study for the City of Knoxville, Tennessee.

3.1. Parameters Estimated From the Literature

In the following, we use the literature and industry reports to estimate model parameters. Planning horizon, T. In this paper, we use two planning horizons of 10 years and 20 years. These two horizons are chosen based on the availability of future climate projections as well as the lifespan of current commercially available PV panels and GRs.

PV system fixed cost, F, and PV system variable cost in region κ , V^{κ} . The cost of installing PV system includes the workforce cost, plus the costs of the system components, i.e., solar modules (which is referred to the PV cell circuits sealed in an environmentally protective laminate (Florida Solar Energy Center, 2018)), mounting device, DC-AC power inverter, and wiring. Note that both workforce and component costs consist of fixed costs and variable costs, i.e., some of these costs are fixed for any installation, regardless of the size of the PV system, whereas the others are functions of the size of the system. For instance, the workforce cost consists of a fixed cost for engineering design, permit, and contract fees, plus a variable labor cost to install the system. Similarly, the PV system cost consists of a fixed cost for PV modules and mounting device that is a function of the PV system size. In the following, we first calculate the fixed and variable costs of the workforce. Next, we estimate the fixed and variable costs of the PV system components. We then use these values to estimate PV system fixed cost, F, and PV system variable cost in our region of interest, V^{κ} .

According to a 2015 report by the National Renewable Energy Laboratory (NREL) (Chung et al., 2015), installing a 5 kW PV system with a size of 37.5 m² (400 ft²) on a residential rooftop costs \$7,950, which includes the one-time engineering design, permit, and contract

fees, plus the labor costs. In contrast, the cost of installing a commercial system of size 743.2 m² (8000 ft²) equals \$92,132, including the one-time fees and labor costs. We assume the labor costs for installing the PV system increase linearly in the system size, and the one-time fees are equivalent. Let \mathbb{W} denote the total workforce cost needed to install PV system and recall that k_i^{κ} denotes the area of PV panel installed at site $i \in I^{\kappa}$. Hence, using linear regression, we obtain $\mathbb{W} = 3500 + 120k_i^{\kappa}$. Consequently, we use the intercept of \$3,500 and the slope of \$120 per m² as the fixed and variable costs of workforce required for installing a PV system.

Connecting the PV system to the grid requires inverters to convert the direct current (DC) from PV panels into alternating current (AC). These inverters generally cost between \$1,000 and \$5,000 based on their capacity and quality (Solar Quotes, 2017; Wholesale Solar, 2018), with relatively limited additional cost for wiring. In this study, we consider the average cost of \$3,500 for the fixed cost of PV system components, which depending on the brand, is sufficient enough for purchasing inverters with a size of 3,000 W to 12,000 W (Wholesale Solar, 2018). Hence, the PV system fixed cost, F, equals to \$7,000, which consists of the fixed part of total workforce cost, i.e., \$3,500, plus the inverter and wiring costs, i.e., \$3,500.

As of 2017, PV modules cost between \$0.85 and \$1.5 per W. That is, for a panel with the size of 1 m² and 150 W–250 W output on top efficiency, the module cost ranges from \$128 to \$375, while the mounting device (frame) costs an additional \$60 per m². Therefore, the PV system variable cost, V^{κ} , for the City of Knoxville, including the variable part of workforce cost, i.e., \$120 per m², plus module and mounting device cost, ranges between \$310 and \$560 per m².

PV panel output, Q. Commonly available PV panels have an efficiency ranging from 13.5% to 20% (Chung et al., 2015). Therefore, the real output of 1 m² panel during an hour of peak sunlight ranges from 135–200 W.

Total maintenance cost per m^2 PV panel installed in region κ , \mathbb{C}^{κ} . PV panels are made of tempered glass, making them able to withstand harsh weather conditions. Moreover, PV panels have no moving parts, except for panels with tracking mounts, making them very reliable and able to continue operation with minimal maintenance (Boston Solar, 2018). Most

PV panel manufacturers guarantee their products for 20 to 25 years (Whaley, 2016). Therefore, if PV panels cease working, the PV panel companies will fix the issue at no cost. However, in order to utilize PV panels on their full potential, the surface of PV panels should be cleaned throughout their lifespan, which imposes an annual cleaning cost of \$0.25 to \$1.5 per panel (Whaley, 2016), or equivalently \$0.15 to \$0.92 per m² of panel (Energy Saving Trust, 2015). Note that these costs do not consider the positive impact of GRs on reducing air borne pollutants and dust in GR integrated PV panels (Green Roof Technology, 2018).

Recall that in this study we use two planning horizon lengths, i.e., T=10 and T=20 years. Hence, assuming that the current estimated maintenance costs of \$0.15 to \$0.92 per m² of panel increase with inflation, we consider the total maintenance \mathbb{C}^{κ} , incurring in the beginning of the planning horizon, to range between \$1.5 and \$9.2 when T=10 years and between \$3 and \$18.4 when T=20 years.

Average hourly electricity consumption for space conditioning at site i in region κ , H_i^{κ} . Generally speaking, electricity consumption increases in building size (EIA, 2017c). We use the data available from a 2009 survey by the EIA (EIA, 2017c) to characterize the relationship between the average hourly energy consumption for space conditioning and building size. Note that we consider a residential level of energy consumption for all the candidate sites in this study. The data suggests a strong linear relationship between the energy consumption and the building size, where it ranges between 25 m² and 400 m². Recall that A_i^{κ} denotes the available rooftop surface at candidate site i. We assume that the total size of each building is equal to its available rooftop surface, and each candidate site corresponds to a single unit. Hence, the relationship can be best approximated as

$$H_i^{\kappa} = 0.508 + 0.004 A_i^{\kappa}. \tag{10}$$

(For further details about the data and model, please refer to Appendix A.)

Cost per m^2 for installing GR in region κ , P^{κ} . GRs are typically classified into three main types, namely, extensive, semi-intensive, and intensive, mainly based on their types of vegetation and properties, such as weight, use, and maintenance (IGRA, 2017). In this study,

consistent with the existing literature that focuses on energy saving aspect of GRs, we only consider extensive GR, which is the least expensive and most resilient type of GR (Coma et al., 2016; Refahi and Talkhabi, 2015; Dunec, 2012). According to the U.S. General Services Administration (GSA), the cost per m² of extensive GR is approximately \$12 (GSA, 2011) which includes the drainage layer cost as well as labor cost. Consistent with published reports, we do not consider setup costs for GRs (GSA, 2011).

Price per kWh sold to the grid, and cost per kWh purchased from the grid, γ and μ , respectively. Selling excess electricity generated to the grid and being paid in return (Feed-in Tariffs, 2018), known as feed-in tariffs, or more specifically export tariffs (Feed-in Tariffs, 2018), is not generally offered in the U.S., except in a limited number of states (Energy Informative, 2014). However, net metering, which allows for sending the extra electricity generated to the grid at normal retail value and receiving credit for it, is supported by most utility providers (SEIA, 2018). Therefore, consistent with these methods, we consider the same value for the electricity sold to and purchased from the grid as we assume the excess electricity that is sent to the grid can be credited and hence, used by any of the candidate sites. According to EIA (2017), as of 2017, each kWh of electricity purchased from the grid costs approximately 10.3 cents. Hence, we set μ and γ equal to 10.3 cents.

Percentage energy saving in cooling degree-hours due to GR installation, α , and percentage energy saving in heating degree-hours due to GR installation, β . The percentage of energy saving in cooling degree-hours achieved due to the installation of GRs differs across various studies, ranging from 10% to 16.7% (Coma et al., 2016; Dunec, 2012; Ascione et al., 2013; Zhao and Srebric, 2012; Feng and Hewage, 2014; Spala et al., 2008; Raji et al., 2015). While almost all studies agree on the fact that using GRs results in savings in cooling degree-hours, there is a lack of consensus on the impact of GRs in heating degree-hours. Indeed, a few empirical studies report that using GRs contribute to energy loss in heating degree-hours while others suggest that it results in energy savings. For instance, a recent, long-term study reports that GRs increase the required amount of energy to heat the space to a comfortable level (i.e., 22 degrees Celsius in this study) in heating degree-hours by 6.2% (Coma et al., 2016). Consistently, another study performed in different climates throughout

Europe reports up to 1% GR-related energy loss in cold seasons in certain climates (Ascione et al., 2013). In contrast, two empirical studies suggest that the energy savings from GR in heating degree-hours is negligible and can be ignored (Feng and Hewage, 2014; Spala et al., 2008). However, there exists another group of studies that report reductions of 4% to 10% in energy savings as a result of GRs in heating degree-hours (Dunec, 2012; Ascione et al., 2013; Raji et al., 2015; Zhao and Srebric, 2012). Therefore, in this study, we let α and β assume a wide range of values to capture the different, and sometimes contradicting, estimates reported in the literature. Specifically, we let α range from 10% to 20% and β range from -10% to 10%.

Percentage efficiency increase in the output of PV panels due to integration with GRs, θ.

As the results from the previous studies show, integrating PV panels with GRs results in a higher panel efficiency, mainly due to the cooling effect of GRs. However, these studies report a relatively wide range of values for the percentage efficiency increase, i.e., from 3.33% to 8% (Chemisana and Lamnatou, 2014; Hui and Chan, 2011).

Percentage change in energy consumed for space conditioning over the planning horizon, δ . In general, changes in human behavior with respect to energy consumption is not always easily quantifiable and can be impacted by various technological, sociological, climatic, and economic factors (Hostick et al., 2014; Hand, 2012). Over the past few decades, the level of energy consumption for space conditioning in the U.S. residential sector has experienced a steady decline, decreasing from 58% of overall energy consumption per household in 1993, to 48% in 2009 (EIA, 2018a). The projections for the energy consumption for space conditioning, on the other hand, are mixed (EIA, 2018b; Hostick et al., 2014). Published studies report various degrees of increase/decrease in the level of energy consumption for space heating and cooling (Rosenthal et al., 1995; Amato et al., 2005; Mansur et al., 2005; Belzer, 2009; Huang, 2006; Loveland and Brown, 1996; Scott et al., 2005; Ruth and Lin, 2006; Sailor, 2001; Sailor and Pavlova, 2003). For instance, Scott et al. (2005) project the decrease of 24% in the level of energy consumption for space heating and the increase of 39% in the level of energy consumption for space cooling by year 2020. In other studies, Huang (2006) and Amato et al. (2005) project the decrease of as much as 33% and 13% in the level of

Parameter	Ranges	Levels	Sources
PV system variable cost, V^{κ} (USD)	[210, 435]	100, 200, 400, 600	Chung et al. (2015)
Annual maintenance cost per m ² PV panel installed in region κ , $\frac{\mathbb{C}^{\kappa}}{T}$ (USD)	[0.15, 0.92]	0.15, 0.62, 0.92	(Boston Solar, 2018; Whaley, 2016)
PV panel output, Q (W) Percentage energy saving in cooling degree-hours due to GR installation, α	[135, 200] [10%, 16.7%]	100, 200 10%, 20%	Chung et al. (2015); Solar Quotes (2017) Ascione et al. (2013); Coma et al. (2016); Dunec (2012); Feng and Hewage (2014); Raji et al. (2015); Spala et al. (2008); Zhao and Srebric (2012)
Percentage energy saving in heating degree-hours due to GR installation, β	[-6.1%, 10%]	-10%, 10%	Ascione et al. (2013); Coma et al. (2016); Dunec (2012); Feng and Hewage (2014); Raji et al. (2015); Spala et al. (2008); Zhao and Srebric (2012)
Percentage efficiency increase in the output of PV panels due to integration with GRs, θ		2.5%, 10%	Chemisana and Lamnatou (2014); Hui and Chan (2011)
Percentage change in energy consumed for space conditioning over the planning horizon, δ	. , ,	-60%, -40%, -20%, 0%, 20%, 40%, 60%	Amato et al. (2005); Belzer (2009); EIA (2018b,a); Huang (2006); Loveland and Brown (1996); Mansur et al. (2005); Rosenthal et al. (1995); Ruth and Lin (2006); Sailor (2001); Sailor and Pavlova (2003); Scott et al. (2005)

Table 2: Parameter values estimated from the literature and industry reports.

energy consumption for space heating, and the increase of as much as 158% and 40% for space cooling by years 2080 and 2030, respectively. Note that according to EIA (2017c), only a quarter of the total energy consumed for space conditioning in the U.S. residential sector is used for space cooling, while the remaining three quarters is used for space heating. Hence, in this study to capture a wide array of variability, we use a weighted average of the reported values for space heating and cooling, and consequently, account for up to 60% change in total energy consumption for space conditioning.

Initial budget available for investment, B. The net budget for 2017-2018 for the City of Knoxville is equal to \$378.8 million. The City dedicates a fraction of the budget to various long-term urban development projects. For instance, in the 2017-2018 budget, \$17.8 million is dedicated to the conversion of approximately 300,000 street lights across the City to the LED technology, for which the payback period is anticipated to be less than a decade (The City of Knoxville, 2018). Consistent with the budget allocated to this project and other investments in green technologies, in our case study, we set the initial budget available for investment, B, equal to \$20 million.

Table 2 summarizes the parameters that are calibrated from the literature and considered in our numerical studies. The table presents the ranges of values obtained from the literature. In our numerical studies, however, we capture a range slightly larger than the reported values to account for additional uncertainty and possible parameter estimation errors. We conduct our numerical studies at the discrete levels provided in the table.

3.2. Parameters Estimated From Data

390

To estimate the remaining parameters, we use a few datasets including climate projections and solar insolation provided by UDI (UDI, 2017) and CCSI (CCSI, 2017). Total number of cooling degree-hours, $\lambda_{\omega}^{\kappa}$, and heating degree-hours, τ_{ω}^{κ} , in region κ under scenario ω over the planning horizon. The climate system evolves as a result of slow changes in boundary conditions, physical parameters, ocean and sea ice, etc. (IPCC, 2017). General circulation models (GCMs) are climate models which exploit the general circulation mathematical model of a planetary atmosphere (atmospheric GCMs) or ocean (oceanic GCMs) to numerically simulate and project changes in Earth's climate system. Coupled GCMs (CGCMs) consist of models that combine atmospheric GCM (AGCM) with oceanic GCM (OGCM) into interactive ocean-atmosphere models (Yongqiang et al., 2004). In this study, we use the climate projections from ten CGCMs as listed in Table 3. The available projections consist of daily precipitation as well as minimum and maximum temperatures for 1 km² and 4 km² grids for the City of Knoxville from January 2011 through December 2050. In this study, we use the data for two planning horizons of length T=10 years and T=20years, starting from January 2011. In order to reduce the computational effort, we use each climate projection as a scenario in our model, after averaging the daily projections for all grids spanning the City of Knoxville. We examine the impact of using the exact projections for each grid on the results in Section 4.3.

Note that the ten CGCMs are based on similar empirical or theoretical assumptions, hence they are somewhat correlated (Jun et al., 2008). However, as discussed in Section 1, the projected daily temperatures and precipitation values vary across the ten CGCMs. Table 4 presents the maximum, average and the range of standard deviation for daily pairwise

Model	Institute of development
	Meteorological Research Institute of the Japan Meteorological
Climate Model (MRI-CGCM3)	Agency (JMA, 2017)
Max-Planck-Institute Earth System Model Mixed Resolu-	Max Planck Institute for Meteorology (MPI, 2017)
tion (MPI-ESM-MR)	
	Geophysical Fluid Dynamics Laboratory (Princeton University,
Model (GFDL-ESM2M)	2017)
The Australian Community Climate and Earth System	Commonwealth Scientific and Industrial Research Organiza-
Simulator (ACCESS)	tion (CSIRO, 2017)
The NCAR's Community Climate System Model (CCSM4)	Climate and Global Dynamics Laboratory at the National Center
	for Atmospheric Research (NCAR, 2017)
The Institute Pierre Simon Laplace Climate Model (IPSL-	Institute Pierre Simon Laplace (IPSL, 2017)
CM5A)	
The Beijing Climate Center Climate System Model (BCC-	Beijing Climate Center, China Meteorological Administra-
CSM)	tion (BCC, 2017)
Norwegian Earth System Model (NorESM1-M)	Multi-institutional, Coordinated Climate Research in Nor-
	way (EarthClim, 2017)
The Centro Euro-Mediterraneo sui Cambiamenti Climatici	Euro-Mediterranean Center on Climate Change (CMCC, 2017)
Climate Model (CMCC-CM)	
Flexible Global Ocean Atmosphere Land Sys-	Institute of Atmospheric Physics, Chinese Academy of Sciences,
tem (FGOALS)	State Key Laboratory of Numerical Modeling for Atmospheric
	Sciences and Geophysical Fluid Dynamics (LASG, 2017)

Table 3: Ten coupled general circulation models (CGCMs) generated at Oak Ridge National Laboratory's Climate Change Science Institute (CCSI, 2017) using high-performance computing resources, including Titan, America's fastest supercomputer (CCSI, 2017).

comparisons across the ten projections over the given planning horizon. As seen in Table 4, the average value of the pairwise differences for daily maximum and minimum temperatures for both T=10 years and T=20 years are on the order of 5 degrees Celsius, which highlight the existing variations in the projected values. (For detailed plots on daily/monthly/yearly average temperatures for the City of Knoxville, Tennessee for the ten different climate projections, please see Appendix B.)

		T=	=10	T=20				
Parameter	Maximum	Average	Standard deviation range	Maximum	Average	Standard deviation range		
Daily maximum temperature (°C)	30.63	4.71	[0.89,7.95]	31.41	4.72	[0.79,7.95]		
Daily minimum temperature (°C)	41.58	4.82	[0.47, 11.13]	41.58	4.79	[0.47, 11.22]		
Daily precipitation (mm)	105.26	5.40	[0.02, 38.88]	105.26	5.45	[0.02, 38.88]		

Table 4: Maximum, average and the standard deviation range for daily pairwise comparisons across the projections from ten CGCMs, presented in Table 3, over two planning horizons of length T=10 years and T=20 years, starting from January 2011.

As discussed, the data generated by CGCMs are on a daily basis. However, to accurately calibrate the model formulated in Section 2, we require hourly data. Hence, we

use the widely accepted cosine function to disaggregate the temperature data into hourly predictions (Green and Kozek, 2003), i.e.,

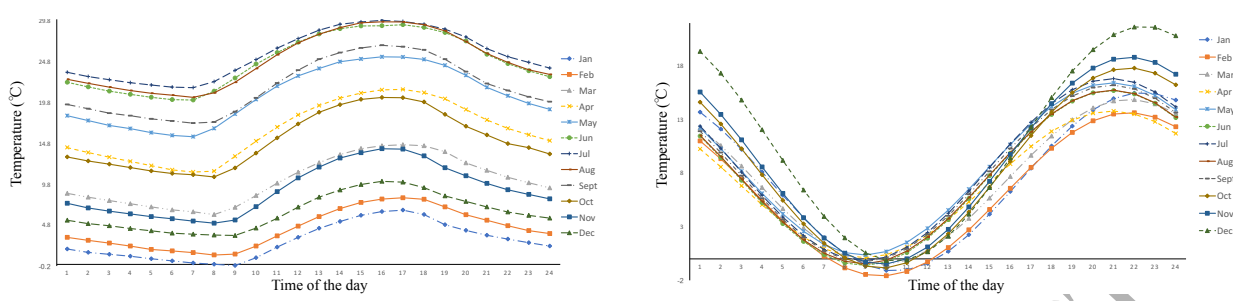
$$Y_t = a\cos\left(\frac{\pi(t+b)}{12}\right) + c + \epsilon. \tag{11}$$

Using this function requires daily minimum and maximum temperatures, and the time of the day during which these extreme temperatures occur. Hence, to estimate these data points, we use the hourly historical data from 2010 to 2012 provided by McGhee Tyson Airport weather station in Knoxville (CRONOS, 2017), to obtain the time at which the daily minimum and maximum temperatures were previously observed. As shown in Figure 3a, the daily minimum and maximum temperatures occur at different times during the day dependent on the month of the year. For instance, in the month of May, the daily minimum and maximum temperatures on average occur at 7 A.M. and 4 P.M., respectively, while in January, the daily minimum and the maximum temperatures on average occur at 9 A.M. and 5 P.M., respectively. Figure 3b shows the hourly temperatures for ACCESS CGCM obtained from Equation (11) and calibrated with the data presented in Figure 3a. The same approach is used to obtain the hourly temperatures from the remaining nine CGCMs.

In order to estimate the total number of cooling and heating degree-hours during a given day, we need cut-off values to guide when cooling and heating are required. Recommended comfort human temperatures are often reported as 20-23.3 degrees Celsius in winter and 22.8 to 25.6 degrees Celsius in summer (Burroughs and Hansen, 2013). A 2009 survey conducted by the EIA (EIA, 2018b) shows that in the U.S., residential households usually use space conditioning for heating and cooling when the outdoor temperature ranges between 14.4 and 17.8 degrees Celsius, and 17.8 and 19.4 degrees Celsius, respectively. In this study, consistent with the recent published works, we set the cut-off values for heating and cooling degree-hours to 22 and 18 degrees Celsius, respectively (Coma et al., 2016; Degree Days Weather Data, 2017).

430

Total number of peak sunlight hours available in region κ under scenario ω over the planning horizon, L_{ω}^{κ} . Our datasets report projected temperature and precipitation, but do not



- (a) The hourly temperatures in a day, averaged across (b) The ACCESS CGCM projected hourly tempermonth of the year from 2010 to 2012 based on the atures in a day, averaged across month of the year historical data (CRONOS, 2017).
 - from 2011 to 2021, obtained using Equation (11).

Figure 3: Example hourly temperature values for the City of Knoxville

include the daily peak sunlight hours. Also note that the number of daily peak sunlight hours is different from the readily available number of daily sunlight hours (Solar Direct, 2017). Hence, we use the amount of daily precipitation to estimate the total number of peak sunlight hours available, L_{ω}^{κ} . Specifically, we assume that any day with a precipitation greater than 10 mm is a cloudy day, and hence no peak sunlight hour is considered for such days. We obtain the estimate of 10 mm by comparing the results for the years 2011 and 2012 with the annual average peak sunlight hours (Current Results Weather and Science Facts, 2017).

Rooftop radiation potential, ι_i^{κ} , rooftop surface available, A_i^{κ} , at site i in region κ , and total energy requirement for space conditioning in region κ over the planning horizon, R^{κ} . To obtain rooftop radiation potential, we use the solar insolation dataset provided by UDI (UDI, 2017) and CCSI (CCSI, 2017). This dataset includes the information about the rooftop size and solar insolation for 209,183 buildings in the City of Knoxville for the year 2003. The model that produces the data uses GIS and high-resolution Light Detection And Ranging (LiDAR) data to generate solar radiation intensity values for each building (Kodysh et al., 2013). This high spatial and temporal resolution dataset is depicted in Figure 4. As seen in Figure 4, large rooftops generally have high solar insolation values mainly due to their flat surface and unobstructed access to the sunlight.

To estimate the values of ι_i^{κ} , we first obtain the per m² solar insolation values by dividing the solar insolation value of each rooftop by the size of the rooftop (in m²). We then rescale them to range between 0 and 1.

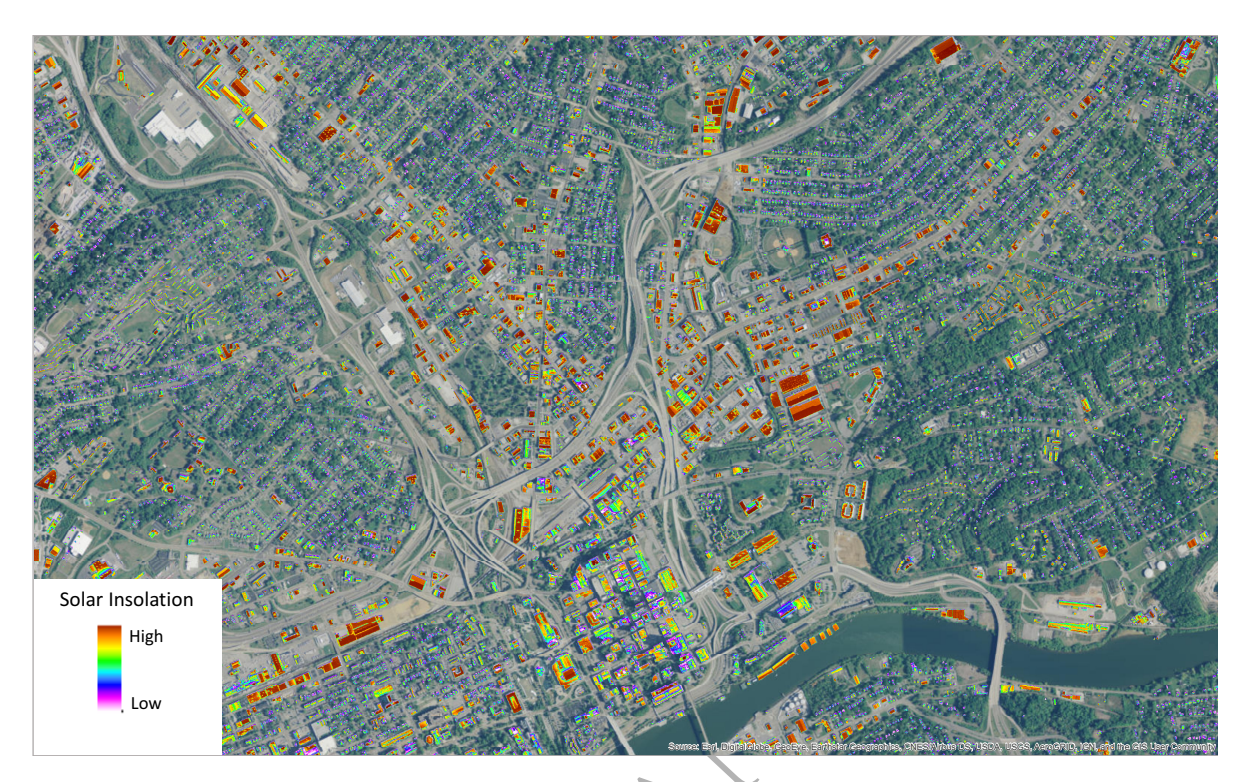


Figure 4: Visual-SOLAR radiation map for the City of Knoxville, Tennessee (Kodysh et al., 2013).

NREL (Gagnon et al., 2016) defines three categories for building sizes, i.e., small (with rooftop sizes less than 185 m²), medium (with rooftop sizes between 185 m² and 2,500 m²), and large (with rooftop sizes larger than 2,500 m²). Figures 5a and 5b respectively show the distribution of rooftop sizes and solar insolation values for the 209,183 buildings in the City of Knoxville. As seen in Figure 5b, in general, the larger the building, the larger the solar insolation value.

Recall that in Section 3.1, we assume that the total size of each building is equal to its available rooftop surface, and each candidate site corresponds to a single unit. Accordingly, Equation (10) approximates the relationship between the available rooftop surface at a given candidate site and the corresponding average hourly electricity consumption for space conditioning at that site. Hence, based on the data provided by Kodysh et al. (2013), we estimate the total energy requirement for space conditioning in the City of Knoxville to be approximately equal to 6.4 million GWh and 12.8 million GWh for T = 10 and T = 20, respectively. The realization probability of scenario ω , η_{ω} . In this study we use the climate projections

475

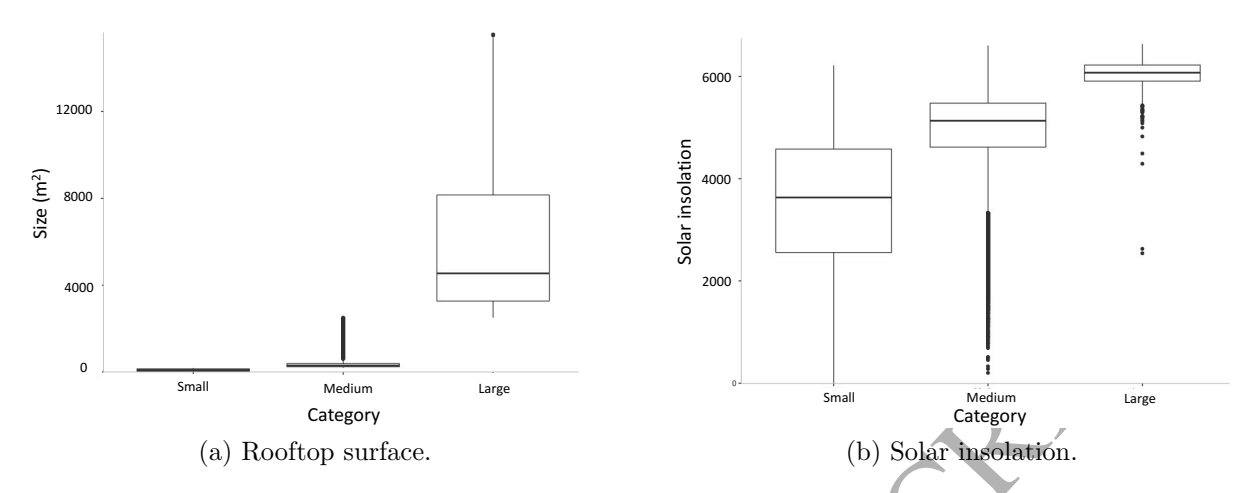


Figure 5: Rooftop size and solar insolation for the 209,183 buildings in the City of Knoxville, stratified across rooftop size category.

discussed earlier in this section as our scenarios. The parameter η_{ω} gives the likelihood that a scenario is realized. As discussed, climate projections can be correlated (Jun et al., 2008). However, due to the lack of information about the exact development process of the CGCMs, here we assume that all scenarios are equally probable, i.e., $\eta_{\omega} = 0.1 \,\forall \omega \in \Omega$.

80 4. Computational Study

In this section, we provide extensive numerical results. First, we discuss the solution approach and introduce additional metrics in Section 4.1. Next, in Section 4.2 we provide a case study and discuss the results. Next, in Sections 4.3 and 4.4, we conduct extensive sensitivity and robustness analyses on model parameters, respectively, and provide insights. Finally, in Section 4.5 we discuss the environmental implications of the optimal solutions obtained in the case study.

4.1. Solution Approach and Additional Metrics

We use the L-shaped decomposition algorithm (Van Slyke and Wets, 1969) to efficiently solve the problem. In order to implement this method, we linearize Equation (6). To remove the non-linearity caused by $k_i^{\kappa} y_i^{\kappa}$, we employ the big M method (Griva et al., 2009). We add

two new continuous variables $\zeta_i^{1\kappa}$ and $\zeta_i^{2\kappa}$ to the model such that

$$\zeta_i^{1\kappa} + \zeta_i^{2\kappa} = k_i^{\kappa}, \qquad \zeta_i^{1\kappa} \le M y_i^{\kappa}, \qquad \zeta_i^{2\kappa} \le M (1 - y_i^{\kappa}) \qquad \forall i, \kappa, \tag{12}$$

where M is a sufficiently large number. We add the set of constraints in Equation (12) to the model and replace Equation (6) with the following set of constraints:

$$e_{i\omega}^{\kappa} = Q L_{\omega}^{\kappa} k_{i}^{\kappa} \iota_{i}^{\kappa} + Q L_{\omega}^{\kappa} \iota_{i}^{\kappa} \zeta_{i}^{1\kappa} \theta \qquad \forall i, \omega, \kappa.$$

$$(13)$$

In the following we introduce two new metrics. These metrics are used to facilitate the comparison of the results.

Return on investment, ROI. Recall that our objective is to maximize the overall profit from energy generated and saved. However, to more easily compare the efficiency of the prescribed investment options, we introduce this new metric. Specifically, return on investment is calculated by dividing the net profit by the cost of investment multiplied by 100, i.e.,

$$ROI = \frac{\sum_{i} \sum_{\kappa} -(Fx_{i}^{\kappa} + k_{i}^{\kappa}V^{\kappa} + A_{i}^{\kappa}P^{\kappa}y_{i}^{\kappa}) + \sum_{\omega} \sum_{i} \sum_{\kappa} \eta_{\omega}(e_{i\omega}^{\kappa} + s_{i\omega}^{\kappa})}{\sum_{i} \sum_{\kappa} (Fx_{i}^{\kappa} + k_{i}^{\kappa}V^{\kappa} + A_{i}^{\kappa}P^{\kappa}y_{i}^{\kappa})} \times 100.$$
 (14)

Sustainability index, SI. As discussed in Section 1, one of the major intangible, non-financial benefits associated with using PV panels and GRs is reducing the reliance on fossil fuels. This metric quantifies the percentage of the requisite energy that is saved or generated by using GRs and/or PV panels under the optimal solution, i.e.,

$$SI = \frac{\sum_{\omega} \sum_{i} \sum_{\kappa} \eta_{\omega} (e_{i\omega}^{\kappa} + s_{i\omega}^{\kappa})}{\sum_{\kappa} R^{\kappa}} \times 100.$$
 (15)

Although our objective is not to maximize SI, such metric can help policy makers to compare intangible benefits of the provided solutions.

4.2. Case Study

510

In this section, we present the results for a case study for the City of Knoxville, Tennessee. Specifically, we examine a set of 209,183 buildings, as candidate sites in one region, given an initial investment budget of \$20 million. As discussed in the introduction, we take the perspective of a regional governing body throughout this paper. Nonetheless, the model is versatile and can be easily modified and calibrated to study the problem from other perspectives (e.g., utility companies).

Note that an average residential building in the southern U.S. built by 2010 is of size 220 m² (Census Bureau, 2018a) and has 1.5 floors (Census Bureau, 2018b). In this study, to capture the energy savings of GRs which typically only provide energy savings for the top floor unit(s), we assume all buildings are single units.

In order to capture the effects of current prices and efficiency of the PV panels, we consider three cases. In this section, we set $\delta = 0$. We later conduct sensitivity analysis on the impact of parameter δ on the solutions. In these cases, we use the values estimated form the literature and summarized in Table 2. Specifically, in all three cases, we set the percentage energy saving in cooling and heating degree-hours by GRs, i.e., α and β , respectively, equal to 10% and 0%. In Case 1, we consider the price and efficiency of current commercially available panels. That is, we set the PV panel output, Q, and the PV system variable cost in the City of Knoxville, V^{κ} , equal to 0.15 and 400, respectively. As discussed in Section 1 the cost of PV panels is on the decline while their efficiency is increasing. Hence, Case 2 considers efficient PV panels with lower than average cost to capture a likely upcoming scenario. In both Cases 1 and 2 we set the percentage efficiency increase in the output of PV panels due to integration with GRs, θ , equal to 5%. Note that θ is directly related to the ability of GRs to reduce their surrounding environment temperature. In Case 3, we use the range reported in Table 2 to approximate a linear relationship between hourly percentage efficiency increase in the output of PV panels due to integration with GRs and hourly temperature. In this case, unlike Cases 1 and 2 in which we consider a fixed value for θ regardless of the outside temperature, we incorporate the effect of the outside temperature in the GR-provided efficiency increase of PV panels. Let θ_t denote hourly percentage efficiency increase in the

Case study	PV panel output, $Q (kW)$	$\begin{array}{c} \text{PV system} \\ \text{variable cost}, \\ V \text{ (USD)} \end{array}$	Percentage energy saving in cooling degree-hours by GRs, α	Percentage energy saving in heating degree-hours by GRs, β	Percentage efficiency increase in PV panel output, θ
Case 1 Case 2 Case 3	0.15 0.2 0.2	400 200 200	10% 10% 10%	$0.0\% \\ 0.0\% \\ 0.0\%$	$5\% \\ 5\% \\ \theta_t = 0.0013 \mathbb{T}_t + 0.091$

Table 5: The parameter values in the three cases considered in the case study for the City of Knoxville.

output of PV panels due to integration with GRs and \mathbb{T}_t denote the hourly temperature. From the linear regression we obtain $\theta_t = 0.0013\mathbb{T}_t + 0.091$. Applying this function to the climate projections results in θ_t values that range from 0.064 to 0.14, which are larger than θ values considered in both Case 1 and Case 2. Table 5 summarizes the three cases considered.

We use Gurobi Optimizer version 7.5 (Gurobi, 2014) on an iMac Pro with an 8-core 3.2 GHz Intel Xeon W processor and 32 GB of RAM to solve the model. The solution time for the three cases ranges between 422.2 seconds and 463.6 seconds. Appendix C provides further details on the solution time, number of variables, and number of constraints for the three cases.

530

535

Table 6 provides the optimal solutions for the three cases presented in Table 5. In all three cases, the total energy generated/saved is not enough to fully compensate the requisite energy needs of the City of Knoxville for space conditioning, either because of non-profitability of PV panels/GRs or the limited available budget for investment. Hence, in all these cases, the value of the objective function is negative. However, as seen in the table, ROIs are positive, suggesting that the income from the total energy generated/saved is higher than the budget spent.

First, note that when T=10 only a small proportion of the available budget is spent under the optimal solution and only GRs are installed in all three cases. This is mainly due to the fact that when T=10, the amount of electricity generated by PV panels is not nearly enough to cover their installation costs. In addition, because only GRs are installed in these three cases and the values for α and β are identical across the cases, the solutions and the metrics are also the same.

Similarly, when T=20 in Case 1 only GRs are installed under the optimal solution

			T = 10			T = 20						
	Stand-alone PV (m ²)	Stand-alone GR (m ²)	PV+GR (m ²)	Budget spent (\$)	SI	ROI	Stand-alone PV (m ²)	Stand-alone GR (m ²)	PV+GR (m ²)	Budget spent (\$)	SI	ROI
Case 1	0	999	0	11,988	0.0033%	75.82%	0	21,969	0	263,628	0.0283%	37.97%
Case 2	0	999	0	11,988	0.0033%	75.82%	99,612	2,295	0	20,000,000	2.8724%	84.60%
Case 3	0	999	0	11,988	0.0033%	75.82%	0	4,735	93,930	$20,\!000,\!000$	2.8893%	87.72%

Table 6: Optimal solution for an initial budget of \$20 million available for investment over two planning horizons of length T = 10 years and T = 20 years for the cases presented in Table 5.

and not all available budget is spent. However, in Cases 2 and 3, the optimal solution also prescribes to install PV systems and all available budget is allocated. Specifically, in Case 1, 21,969 m² of stand-alone GRs are installed under the optimal solution. Considering the average residential building rooftop size of 145 m² in the southern U.S. (Census Bureau, 2018a), this is enough to cover to approximately 152 average residential buildings. In Case 2, more than 99% of the available budget is allocated to installing 99,612 m² of stand-alone PV panels, and the rest of the budget is allocated to installing 2,295 m² of stand-alone GRs, in total covering an approximately 703 average residential buildings. Note that in this case GRs are not integrated with PV panels; hence, they are mainly installed to provide energy savings. In Case 3, approximately 94% of the budget is allocated to installing PV panels, all of which GR integrated, and the rest is used for installing an additional 4,735 m² of standalone GRs. In total, under the optimal solution, these practices cover an approximately 680 average residential buildings. Recall that estimated percentage efficiency increase in the output of PV panels due to integration with GRs in Case 3 is overall higher than the two other cases. Hence, in Case 3 more budget is allocated to GRs compared to Case 2 and all panels are GR integrated to achieve a higher electricity output. Note that contrary to Case 2, in Case 3 GRs are mainly used to help improve the output of PV panels.

The model generally prescribes the stand-alone GRs to be installed on small rooftops. Recall that Equation (10) presents the relationship between hourly energy consumption for space conditioning and building size. From Equation (10), the magnitude of the intercept is much larger than that of the slope. Therefore, for instance, two small buildings would consume more energy than a large building that has a rooftop area equivalent to the total area of the two small rooftops. Note that the energy savings from GRs are a fraction of the

total energy consumed by the buildings (based on α and β .) Therefore, because GRs do not have a set up cost, when it is optimal to install stand-alone GRs, the model typically prioritizes small rooftops to generate more profit through their energy savings.

In contrast, the model generally prescribes to install PV panels on large rooftops, partially due to the fact that installing PV systems has a fixed set-up cost. Additionally, as discussed in Section 3.2, buildings with large rooftops often have the highest radiation potential, ι_i^{κ} , as they are mostly flat and unlikely to be completely shaded by their surrounding buildings. Hence, the model prioritizes large rooftops for PV installation to minimize the cost while maximizing the electricity generation.

As shown in Table 6, for T=10 years, Cases 1-3 result in the same ROI values as the corresponding solutions are identical. For T=20 years, the solutions vary for the three cases and the highest ROI value is achieved in Case 3 in which the benefit of GRs are most accurately captured. The SI values in Table 6 are generally higher for T=20 years compared to T=10 years, as PV panels are installed for T=20 years.

4.3. Sensitivity Analysis

575

585

In this section, we conduct extensive sensitivity analysis to evaluate the impact of model parameters on the optimal solution. First, we conduct a sensitivity analysis on an array of parameters related to PV panels, GRs, and their interaction. Second, we examine the impact of possible changes in energy consumed for space conditioning over the planning horizon on optimal solutions. Next, we investigate the impact of incorporating maintenance cost directly into the model as a responsibility of the entity in charge of planning, e.g., the regional governing body. Lastly, we evaluate the impact of using the averages of the daily projections over all grids spanning the City of Knoxville, instead of the true projections for each grid, when calibrating the model, and provide recommendations.

Table 7 presents the results from the sensitivity analysis for different levels of PV system variable cost, V^{κ} , PV panel output, Q, percentage efficiency increase in the output of PV panels due to integration with GRs, θ , and percentage energy saving in cooling and heating degree-hours due to GR installation, α and β , respectively, as presented in Table 2. In

general, when PV systems are expensive but have relatively low output, i.e., high V^{κ} values and low Q values, the optimal solution mainly depends on the energy savings from GRs. In this case, if the percentage energy saving in heating degree-hours due to GR installation, β , is low, no additional profit can be generated from installing GRs or PV panels. Hence, the model chooses to not spend any budget at all. When β is high, the model chooses to spend budget but only for stand-alone GRs, mainly to achieve energy savings, and hence maximize the profit. In this case, the total number of stand-alone GRs depends on and increases in the percentage energy saving in cooling degree-hours due to GR installation, α .

For cost-efficient PV systems, i.e., low V^{κ} values and high Q values, the optimal solution mainly depends on the percentage efficiency increase in the output of PV panels due to integration with GRs, θ . That is, when θ is low, the optimal solution is to install standalone PV panels. However, when θ is high, the model takes full advantage of the added efficiency and prescribes to install a large quantity of GR integrated PV panels, with the remaining budget spent on stand-alone GRs. In this case, the proportion of budget spent on stand-alone GRs increases in both α and β .

In general, the length of the planning horizon can significantly impact the optimal solution. For instance, as the highlighted row on Table 7 shows, for T=10 years the optimal solution is to not spend any budget, whereas for T=20 years the optimal solution is to allocate all of the budget to install stand-alone PV panels.

615

Additionally, ROI and SI values are generally higher for T=20 years compared to T=10 years. To eliminate the effect of different planning horizon lengths, we calculate the average annual ROI and SI values for T=10 years and T=20 years by dividing the values in the table by their planning horizon lengths. The results show that for T=20 years the average annual ROI and SI values are at least as large as the average annual values for T=10 years for any combination of parameters. This is mainly due to the higher number of peak sunlight hours and cooling degree-hours during the second decade of the 20-year planning horizon.

Overall, the results from Table 7 show that while the optimal solution of the model relies on the values of the key parameters, the length of the planning horizon, T, plays a significant role in the allocation of the initial investment. Moreover, Table 7 shows that both the per-

						T	'= 10				T	= 20		
PV panel output, Q (kW)	PV system variable cost, V^{κ} (USD)	Percentage energy saving in cooling degree-hours by GRs, α		Percentage efficiency increase in PV panel output, θ		$\begin{array}{c} {\rm Stand\text{-}alone} \\ {\rm GR}~({\rm m}^2) \end{array}$	$^{\rm PV+GR}_{\rm (m^2)}$	SI	ROI	$\begin{array}{c} {\rm Stand\text{-}alone} \\ {\rm PV}~({\rm m}^2) \end{array}$	Stand-alone GR (m ²)	$^{\rm PV+GR}_{\rm (m^2)}$	SI	ROI
		10%	-10%	2.5% 10%	0 0	0 885	0 178,030 0	0.000% 1.965%	0.00% 63.13%	199,400 0	0 885	0 178,030	1.283% 3.508%	82.43% 225.45%
	100		10%	2.5% 10%	0	76,875 14,344	176,410	0.056% 2.031%	38.76% 65.26%	187,087 0	103,443 14,344	176,410	1.356% 3.574%	87.12% 229.68%
	100	20%	-10%	2.5% 10%	0	0 885	0 178,030	0.000% 1.979%	0.00% 63.59%	199,396 0	31 885	0 178,030	1.283% 3.523%	82.43% 226.39%
			10%	2.5% 10%	0	192,650 34,058	0 174,386	0.155% 2.074%	43.22% 66.65%	169,430 0	250,580 34,074	0 174,385	1.480% 3.618%	95.14% 232.52%
		10%	-10%	2.5% 10%	0	0	0	0.000% 0.000%	0.00% 0.00%	0 /	0 2,302	0 94,068	0.000% 1.145%	0.00% 73.62%
	200	1070	10%	2.5% 10%	0 0	76,875 76,875	0	0.056% 0.056%	38.76% 38.76%	0	589,660 104,608	0 88,277	0.270% 1.251%	49.03% 80.43%
	200	20%	-10%	2.5% 10%	0 0	0	0	0.000% 0.000%	0.00% 0.00%	0	137 2,335	0 94,066	0.000% 1.153%	23.42% 74.12%
10%		2070	10%	2.5% 10%	0	192,650 192,650	0	0.155% 0.155%	43.22% 43.22%	0	1,166,725 251,691	0 79,999	0.641% 1.394%	58.85% 89.60%
1070		10%	-10%	2.5% 10%	0	0	0	0.000% 0.000%	0.00% 0.00%	0	0	0	0.000% 0.000%	0.00% 0.00%
	400	1070	10%	2.5% 10%	0	76,875 76,875	0	0.056% $0.056%$	38.76% 38.76%	0	589,660 589,660	0	0.270% 0.270%	49.03% 49.03%
	400	20%	-10%	2.5% 10%	0	0	0	0.000% 0.000%	0.00%	0	137 137	0	0.000% 0.000%	23.42% 23.42%
			10%	2.5% 10%	0	192,650 192,650	0	0.155% 0.155%	43,22% 43.22%	0	1,166,725 1,166,725	0	0.641% 0.641%	58.85% 58.85%
		1007	-10%	2.5% 10%	0	0 0	0	0.000% 0.000%	0.00% 0.00%	0	0	0	0.000% 0.000%	0.00% 0.00%
	200	10%	10%	2.5% 10%	0	76,875 76,875	0	0.056% 0.056%	38.76% 38.76%	0	589,660 589,660	0	0.270% 0.270%	49.03% 49.03%
	600 -	2007	-10%	2.5% 10%	0	0	0	0.000%	0.00%	0	137 137	0	0.000%	23.42% 23.42%
		20%	10%	2.5% 10%	0	192,650 192,650	0	0.155% 0.155%	43.22% 43.22%	0	1,166,725 1,166,725	0	0.641% 0.641%	58.85% 58.85%
		~	-10%	2.5% 10%	199,300	0 885	0 178,030	2.580% 7.054%	82.91% 226.66%	199,300	0 885	0 178,030	4.122% 8.584%	264.89% 551.67%
		10%	10%	2.5% 10%	198,435	8,039 1,589	0 177,955	2.593% 7.110%	83.33% 228.47%	198,435 0	8,039 1,589	0 177,955	4.135% 8.640%	265.72% 555.27%
	100		-10%	2.5% 10%	199,300	0 885	0 178,030	2.580% 7.068%	82.91% 227.12%	199,300	0 885	0 178,030	4.122% 8.598%	264.89% 552.61%
		20%	10%	2.5% 10%	196,007 0	28,274 3,455	0	2.615% 7.128%	84.05% 229.05%	196,007	28,274 3,455	0	4.158% 8.658%	267.20% 556.45%
			-10%	2.5% 10%	0	0 2,302	0 94,068	0.000% 2.311%	0.00% 74.26%	99,750	0 2,302	0 94,068	1.315% 3.853%	
		10%	10%	2.5% 10%	0	76,875 10,824	0 93,585	0.056% 2.351%	38.76% 75.56%	93,643	103,443 10,824	0 93,585	1.386% 3.893%	89.09% 250.22%
	200		-10%	2.5% 10%	0	0 2,302	0 94,068	0.000% 2.319%	0.00% 74.51%	99,748	31 2,302	0 94,068	1.315% 3.861%	84.49% 248.16%
		20%	10%	2.5% 10%	0	192,650 39,001	0 91,849	0.155% 2.381%	43.22% 76.52%	84,815 0	250,580 39,001	0 91,849	1.508% 3.924%	96.88% 252.21%
20%			-10%	2.5% 10%	0	0 0	0	0.000% 0.000%	0.00%	0	0 192	0 48,490	0.000% 1.256%	0.00% 80.74%
		10%	10%	2.5% 10%	0	76,875	0	0.056% 0.056%	38.76% 38.76%	0	589,660 106,739	48,490 0 45,386	0.270% 1.340%	49.03% 86.09%
	400		-10%	2.5%	0	76,875	0	0.000%	0.00%	0	137	0	0.000%	23.42%
		20%	10%	10% 2.5%	0	192,650	0	0.000%	0.00% 43.22%	0	1,166,725	48,489	1.260% 0.641%	80.99% 58.85%
			-10%	10% 2.5%	0	192,650	0	0.155%	43.22% 0.00%	0	251,111	41,181	1.470% 0.000%	94.49%
		10%	10%	10% 2.5%	0	0 76,875	0	0.000%	0.00% 38.76%	0	774 589,660	32,648	0.350%	22.49% 49.03%
	600		-10%	10% 2.5%	0	76,875 0	0	0.056% 0.000%	38.76% 0.00%	0	330,878 137	26,176	0.527% 0.000%	33.89% 23.42%
		20%		10% 2.5%	0	0 192,650	0	0.000% 0.155%	0.00% $43.22%$	0	804 1,166,725	32,648	0.353% 0.641%	22.66% 58.85%
			10%	10%	0	192,650	0	0.155%	43.22%	0	703,127	18,877	0.788%	50.67%

Table 7: Area covered by stand-alone GRs, stand-alone PV panels, and GR integrated PV panels under different values for PV panel output, PV system variable cost, percentage energy saving in cooling and heating degree-hours due to GR installation, and percentage efficiency increase in the output of PV panels due to integration with GRs for an initial budget of \$20 million available over two planning horizons of length T=10 years and T=20 years.

	T = 10							T = 20					
Case study	The rate of energy consumption, δ		Stand-alone GR (m ²)	$^{\mathrm{PV+GR}}_{\left(\mathrm{m}^{2}\right) }$	Budget spent (\$)	SI	ROI	Stand-alone PV (m ²)	Stand-alone GR (m ²)	PV+GR (m²)	Budget spent (\$)	SI	ROI
	-60%	0	137	0	1,644	0.0009%	40.87%	0	629	0	7,548	0.0025%	69.98%
	-40%	0	389	0	4,668	0.0018%	49.60%	0	3,506	0	42,072	0.0077%	41.02%
C 1	-20%	0	629	0	7,548	0.0025%	67.97%	0	8,039	0	96,468	0.0138%	46.60%
Case1	20%	0	3,506	0	42,072	0.0076%	39.35%	0	45,121	0	541,452	0.0478%	36.14%
	40%	0	5,474	0	65,688	0.0104%	41.99%	0	76,875	0	922,500	0.0705%	37.43%
	60%	0	8,039	0	96,468	0.0136%	44.87%	0	116,127	0	1,393,524	0.0947%	39.74%
	-60%	0	137	0	1,644	0.0009%	40.87%	99,792	137	0	20,000,000	7.1776%	84.52%
	-40%	0	389	0	4,668	0.0018%	49.60%	99,777	389	0	20,000,000	4.7856%	84.54%
Case 2	-20%	0	629	0	7,548	0.0025%	67.97%	99,740	999	0	20,000,000	3.5899%	84.57%
Case 2	20%	0	3,506	0	42,072	0.0076%	39.35%	99,422	5,474	0	20,000,000	2.3949%	84.70%
	40%	0	5,474	0	65,688	0.0104%	41.99%	99,268	8,039	0	20,000,000	2.0544%	84.85%
	60%	0	8,039	0	96,468	0.0136%	44.87%	99,051	11,649	0	20,000,000	1.7997%	85.06%
	-60%	0	137	0	1,644	0.0009%	40.88%	0	2,447	94,060	20,000,000	7.2069%	88.59%
	-40%	0	389	0	4,668	0.0018%	49.60%	0	2,715	94,044	20,000,000	4.8064%	88.63%
C 2	-20%	0	629	0	7,548	0.0025%	67.97%	0	2,969	94,030	20,000,000	3.6064%	85.33%
Case 3	20%	0	3,506	0	42,072	0.0076%	39.35%	0	6,019	93,857	20,000,000	2.4116%	87.87%
	40%	0	5,474	0	65,688	0.0104%	41.99%	0	10,824	93,585	20,000,000	2.0694%	86.89%
	60%	0	8,039	0	$96,\!468$	0.0136%	44.87%	0	14,650	93,369	20,000,000	1.8130%	87.18%

Table 8: Area covered by stand-alone GRs, stand-alone PV panels, and GR integrated PV panels under different values of δ , for an initial budget of \$20 million available over two planning horizons of length T=10 years and T=20 years for the cases presented in Table 5.

centage energy saving in cooling and heating degree-hours due to GR installation, α and β , and percentage efficiency increase in the output of PV panels due to integration with GRs, θ , can significantly affect the optimal solution. The values of α and β rely on several different factors, e.g., the type of green media or isolation layer installed, and vary significantly from one climate type to another. Hence, region-specific studies are needed to accurately estimate these parameters before large-scale implementation. In addition, to the best of our knowledge and despite the overwhelming evidence on the benefits of PV-GR integration, these benefits are not completely characterized in the literature. Hence, there is a need to further investigate and quantify this efficiency increase to better justify large-scale investments.

Table 8 presents the results of a sensitivity analysis with respect to percentage change in energy consumed for space conditioning over the planning horizon, δ , using its estimated values as presented in Table 2, for the three cases presented in Table 5. First, note that the optimal solutions presented in Table 8 are more or less consistent with those presented in Table 6, where $\delta = 0$. That is, when T = 10, under the optimal solution, only a small proportion of the available budget is spent and only stand-alone GRs are installed. Also, when T = 20, in Case 1 only a limited number of stand-alone GRs are installed, whereas in

Cases 2 and 3, the majority of the available budget is spent to place stand-alone PV panels and GR integrated PV panels, respectively, and the remaining budget is used for stand-alone GRs. In all three cases, the total area of installed GRs (i.e., stand-alone GRs and GR integrated PV panels) increases in δ , whereas the total area of installed PV panels (i.e., stand-alone PV panels and GR integrated PV panels) decreases in δ . Note that a larger δ means a higher amount of energy consumption over the planning horizon. Hence, when δ is large, GRs, which can save a fraction of the total energy consumed, provide additional benefits compared to PV panels. Therefore, as δ increases, the model allocates a larger portion of the budget to GRs.

It is interesting to note the extent to which the value of δ affects the decisions. For instance, when T=20, the increase in δ drastically increases the total area of installed stand-alone GRs in Case 1, whereas this increase is more modest in Case 2 and especially in Case 3. This is mainly because in Case 1, not all of the budget is allocated. Also, only GRs are economically profitable. Hence, as δ increases, additional GRs are installed to provide further benefit. However, in Case 2, in which all of the budget is already allocated, for stand-alone GRs to be further prioritized over stand-alone PV panels, the energy savings achieved through their installation must be higher than the energy generated by PV panels. Therefore, the increase in δ only modestly increases the area of installed stand-alone GRs. In Case 3, in which again all of the budget is already allocated, PV panels installed enjoy an increase in the output as a result of integration with GRs. Therefore, compared to Case 2, stand-alone GRs face more resistance in being prioritized over GR integrated PV panels, hence a slower growth in the total area of installed stand-alone GRs in this case.

Moreover, for the cases in which all of the budget is spent under the optimal solution, i.e., in Cases 2 and 3 when T=20, SI decreases, whereas ROI increases in δ . Recall that higher levels of δ leads to higher levels of profit through the installation of GRs. Therefore, given the same \$20 million budget, the amount of savings increases in δ , resulting in higher profit and ROI. However, because the amount of increase in GR energy savings is smaller than that of energy consumption, SI decreases in δ .

Lastly, for the cases in which only a small proportion of the budget is spent on installing

			T	= 10				T = 20					
Case study	Annual per m ² PV panel maintenance $\cot, \frac{\mathbb{C}^{\kappa}}{T}$ (\$)	Stand-alone PV (m ²)	$\begin{array}{c} {\rm Stand\text{-}alone} \\ {\rm GR}~({\rm m}^2) \end{array}$	PV+GR (m ²)	Budget spent (\$)	SI	ROI	Stand-alone PV (m ²)	$\begin{array}{c} {\rm Stand\text{-}alone} \\ {\rm GR}~({\rm m}^2) \end{array}$	PV+GR (m ²)	Budget spent (\$)	SI	ROI
	0.15	0	999	0	11,988	0.0033%	75.82%	0	21,969	0	263,628	0.0283%	37.97%
Case 1	0.62	0	999	0	11,988	0.0033%	75.82%	0	21,969	0	263,628	0.0283%	37.97%
	0.92	0	999	0	11,988	0.0033%	75.82%	0	21,969	0	263,628	0.0283%	37.97%
	0.15	0	999	0	11,988	0.0033%	75.82%	98,122	2,295	0	20,000,000	2.8307%	81.93%
Case 2	0.62	0	999	0	11,988	0.0033%	75.82%	94,001	2,295	0	20,000,000	2.7118%	74.28%
	0.92	0	999	0	11,988	0.0033%	75.82%	91,317	3,506	0	20,000,000	2.6372%	69.49%
	0.15	0	999	0	11,988	0.0033%	75.82%	0	6,140	92,525	20,000,000	2.8476%	84.96%
Case 3	0.62	0	999	0	11,988	0.0033%	75.82%	0	4,018	88,876	20,000,000	2.7291%	77.13%
	0.92	0	999	0	11,988	0.0033%	75.82%	0	4,362	86,470	20,000,000	2.6547%	72.41%

Table 9: Area covered by stand-alone GRs, stand-alone PV panels, and GR integrated PV panels under different values of \mathbb{C}^{κ} , for an initial budget of \$20 million available over two planning horizons of length T=10 years and T=20 years for the cases presented in Table 5.

stand-alone GRs under the optimal solution, i.e., Cases 1-3 when T=10 and Case 1 when T=20, the amount of budget spent and SI both increase in δ . This is mainly because higher δ increases the achievable profit through the installation of GRs, making this practice a viable option for a larger number of candidate sites. As a result, a larger proportion of the budget is used to install a larger area of GRs across the candidate sites, leading to higher values of SI.

Table 9 presents the results when maintenance costs are directly incorporated into the model, using the estimated values as presented in Table 2, for the three cases presented in Table 5. First, note that for in all cases when T=10 and in Case 1 when T=20, the results in Table 9 remain the same as those obtained when maintenance costs are assumed to be the property owners' responsibility, presented in Table 6. This is because in these cases, it is not optimal to install PV panels even without incorporating their maintenance costs directly into the model and accounting for PV maintenance costs only makes them a more costly, and hence less favorable, option.

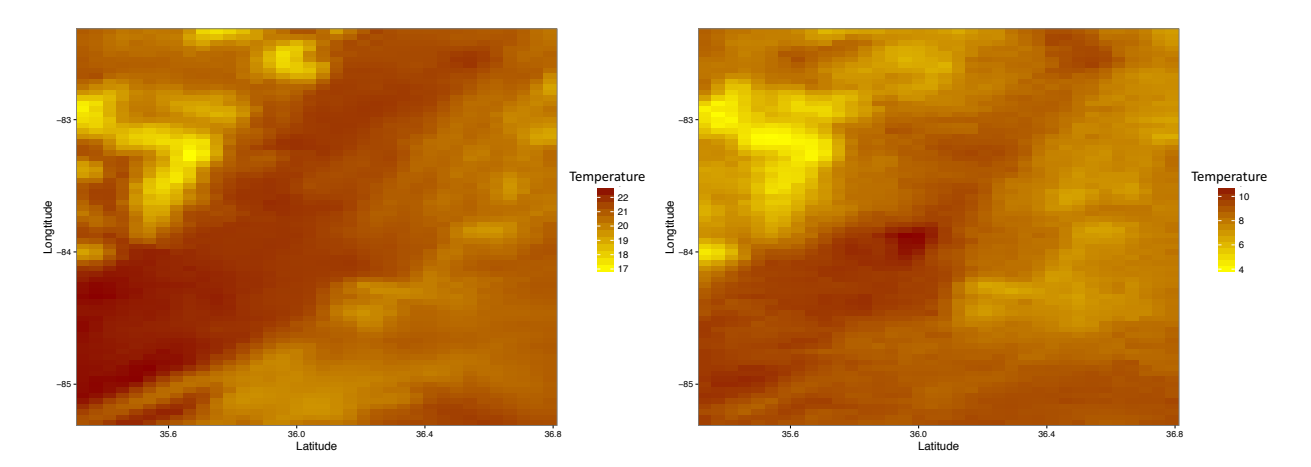
As seen in Table 9, for Cases 2 and 3 when T=20, accounting for PV panel maintenance costs impacts the optimal solutions and negatively affects the ROI and SI metrics. In general, consistent with the intuition, the higher the PV maintenance cost, the more costly the PV panels and hence, the lower the total area of PV panels installed. In particular, in Case 2, when the annual per m^2 PV maintenance cost increases from \$0.15 to \$0.62, stand-alone PV panels become more expensive and the portion of spent budget that is allocated to PV panels results in fewer square meters of PV panels. When the annual per m^2 PV maintenance

cost increases further from \$0.62 to \$0.92, stand-alone PV panels become a less favorable option compared to stand-alone GRs and hence, more of the budget is spent on the latter and the total area of stand-alone PVs drops further. A similar trend is observed for Case 3, in which as the per m² PV maintenance cost increases, GR integrated PV panels become more expensive and consequently, the portion of spent budget that is allocated to PV panels results in fewer square meters of PV panels. However, in this case, GR integrated PV panels generally remain a favorable option despite the increase in their cost. Hence, as the annual per m² PV maintenance cost increases, a larger portion of the budget is allocated to GR integrated PV panels to mitigate the effect of their increased cost. Finally, the remaining portion of the budget that is not spent on installing GR integrated PV panels is allocated to install stand-alone GRs.

Finally, we investigate the impact of using the averages of the daily projections over all grids spanning the City of Knoxville, instead of the true projections for each grid, when calibrating the model. As discussed, the daily temperature projections are generated for grids of sizes 1 km² and 4 km². The daily maximum and minimum temperature projections of the 10 CGCMs show a variation across grids in the City of Knoxville. For instance, Figures 6a and 6b depict the heat map of average daily maximum and minimum temperatures over the year 2030 projected by the ACCESS CGCM across 4-kilometer wide grids for the City of Knoxville. Other climate models show a similar pattern, indicating the variation in the hourly temperatures over different grids.

705

Here, we examine the impact of accounting for the exact projections provided for each grid through a grid-based calibration approach. Specifically, we calculate the total number of cooling and heating degree-hours for each 4 km^2 grid separately, assign each candidate site with the parameters of their corresponding grid, and then resolve the model. Table 10, which is analogous to Table 6, presents the optimal solution for two planning horizons of length T=10 years and T=20 years for the three cases presented in Table 5. As seen in the table, more GRs are installed under the grid-based calibration approach. For instance, in Case 1 for T=20 years, the optimal solution prescribes to increase the total area of stand-alone GRs installed by 80%. This is due to the fact that most of the small



- (a) Average daily maximum temperature.
- (b) Average daily minimum temperature.

Figure 6: Heat map for average daily maximum and minimum temperatures over the year 2030 projected by the ACCESS CGCM across 4-kilometer wide grids for the City of Knoxville.

	T = 10					~ ~		T = 20				
	Stand-alone	Stand-alone	PV+GR	Budget	SI	ROI		Stand-alone	PV+GR	Budget	C1	ROI
	$PV (m^2)$	$GR (m^2)$	(m^2)	spent	51	1001	$PV (m^2)$	$GR (m^2)$	(m^2)	spent	51	1101
Case 1	0	2,813	0	33,756	0.0076%	43.98%	0	39,551	0	474,612	0.0505%	36.75%
Case 2	0	2,813	0	33,756	0.0076%	43.98%	99,521	3,818	0	20,000,000	2.8736%	84.68%
Case 3	0	2,813	0	33,756	0.0076%	43.98%	0	5,989	$93,\!859$	20,000,000	2.8941%	87.83%

Table 10: Optimal solution for an initial budget of \$20 million available for investment over two planning horizons of length T=10 years and T=20 years for the cases presented in Table 5 under the grid-based calibration approach.

and medium buildings in the City of Knoxville are located in the warmer grids and they are assigned a higher number of cooling degree-hours under the grid-based calibration approach. Hence, by installing more GRs the model can achieve more energy savings and consequently a higher profit. The increase in energy savings is also reflected in the SI values. The highest percentage of increase in SI values is equal to 2.22% for Case 1 when T=20 years, which translates into 276.5 GWh of energy saved and generated through sustainable resources.

In general, the grid-based calibration approach provides more accurate representation of the problem at hand. However, the solution provided in Table 10 is relatively consistent with that of Table 6. Hence, considering that the data pre-processing for the grid-based calibration approach is much more computationally expensive, it may or may not be beneficial to use the grid-based calibration approach depending on the specific characteristics of the

region of interest.

740

$_{5}$ 4.4. $Robustness\ Analysis$

As discussed earlier, limited data is available for estimating some of the important model parameters. Hence, it is not unlikely that these parameters are wrongly estimated during implementation. In this section, we conduct robustness analysis to investigate the impact of parameter misspecification on the solution. Specifically, we evaluate the robustness of the model with respect to parameters α , β , and θ , for T=10 and T=20 years, and provide the expected loss of profit due to parameter misspecification.

Let Z^* denote the total profit generated in USD given the true parameter settings. Let \hat{Z} denote the total profit generated in USD from executing the model under extreme parameter misspecifications. Recall that Table 2 provides the estimated parameter ranges and levels used in the study. Hence, \hat{Z} gives the total profit generated when a subset of parameters have been misspecified in the extreme, i.e., the parameters of interest assume their maximum (minimum) values as reported in Table 2, while the true parameter values are at their minimum (maximum). We let \hat{x}_i^{κ} , \hat{y}_i^{κ} , and \hat{k}_i^{κ} denote the corresponding solution. Now let \tilde{Z} denote the total profit in USD when the solution \hat{x}_i^{κ} , \hat{y}_i^{κ} , and \hat{k}_i^{κ} is evaluated under the true parameter values. Lastly, let \tilde{O} denote the cost of misspecifying the parameters, i.e., $\tilde{O} = Z^* - \tilde{Z}$.

Table 11 presents the robustness analysis results on the three parameters of percentage energy saving in cooling degree-hours due to GR installation, α , percentage energy saving in heating degree-hours due to GR installation, β , and percentage efficiency increase in the output of PV panels due to integration with GRs, θ , for an initial budget of \$20 million available over two planning horizons of length T=10 years and T=20 years. The parameters α , β , and θ are particularly chosen as they are generally difficult to estimate and are functions of many other factors themselves, such as the type of GR vegetation, the GR isolation layer, and the climate. As seen in Table 11, the lost opportunity, \tilde{O} , ranges between \$275 thousand and \$12.4 million. Note that for T=10, the values of \tilde{O} are not impacted by the change in the value of θ as no PV panel is installed in these cases. Overall, despite

Planning horizon, T	Percentage energy saving in cooling degree-hours by GRs, α	Percentage energy saving in heating degree-hours by GRs, β	Percentage efficiency increase in PV panel output, θ	Z^* (USD)	$ ilde{Z}$ (USD)	\tilde{O} (USD)
		-10%	2.5% 7.5%	(642,680,064) (642,680,064)	(642,306,584) (642,306,584)	373,480 373,480
	10%	10%	2.5% 7.5%	(644,895,574) (644,895,574)	(642,680,064) (642,680,064)	2,215,510 2,215,510
10	20%	-10%	2.5% 7.5%	(642,680,064) (642,680,064)	(642,405,147) (642,405,147)	274,917 274,917
		10%	2.5% 7.5%	(645,583,951) (645,583,951)	(642,680,064) (642,680,064)	2,903,887 2,903,887
	1004	-10%	2.5% $7.5%$	(2,441,792,744) (2,442,331,322)	(2,437,914,658) (2,438,457,551)	3,878,086 3,873,771
20	10% -	10%	$2.5\% \\ 7.5\%$	(2,446,274,934) (2,446,791,546)	(2,441,402,503)	4,872,431 4,998,802
20	20%	-10%	$2.5\% \\ 7.5\%$	(2,441,792,744) (2,442,412,330)	(2,439,849,247) (2,440,445,560)	1,943,497 1,966,770
		10%	2.5% $7.5%$	(2,453,838,358)	(2,441,483,511) (2,441,792,744)	12,354,847 12,427,434

Table 11: Robustness analysis for different parameter combinations for an initial budget of \$20 million available over two planning horizons of length T = 10 years and T = 20 years. Negative values are enclosed in parentheses.

the significant difference among the values of \tilde{O} in the table, this difference is somewhat small with respect to θ , when all other parameters are held constant. The values of \tilde{O} are in general most sensitive with respect to the parameters α , and especially β , and hence, care needs to be taken when calibrating these parameters for an investment in a particular climatic region.

4.5. Environmental Insights

Recall that the goal of the model is to maximize the overall *profit* from energy generated and/or saved across a set of regions by investing in PV systems and/or GRs. In this section, we discuss the environmental implications of such an investment and provide insights on the benefits achievable by the implementation of the proposed model.

			T = 10		T = 20			
		Coal (kg)	Natural gas (m ³)	Oil (m ³)	Coal (kg)	Natural gas (m ³)	Oil (m ³)	
C	ase 1	101,275	44,104	61	1,747,690	761,092	1,044	
C	ase 2	$101,\!275$	44,104	61	$176,\!663,\!933$	76,934,444	$105,\!564$	
C	lase 3	$101,\!275$	44,104	61	$179,\!670,\!700$	78,243,845	$107,\!361$	

Table 12: Total amount of requisite fossil fuels to produce the electricity saved and/or generated under the optimal solution in Cases 1–3 for two planning horizons of length T=10 years and T=20 years.

Table 12 presents the positive impact of implementing the optimal solutions provided for the three cases introduced in Table 5, for T=10 years and T=20 years, from an environmental perspective. Specifically, Table 12 presents the amount of fossil fuels needed (EIA, 2017a) to produce the amount of electricity that is generated and/or saved through the implementation of the solutions provided in Table 6, after accounting for the required energy for manufacturing, distribution, and end-of-life processing of installed PV panels (Bankier and Gale, 2006; Alsema and Nieuwlaar, 2000; EIA, 2018c; Frischknecht et al., 2015). Note that the corresponding required energy for GRs are negligible (Bianchini and Hewage, 2012). (Please see Appendix D for more detail.)

For instance, consider Case 3 in Table 6. When T=20 years, it is optimal to install 4,735 m² stand-alone GRs and 93,930 m² GR integrated PV panels. As shown in Table 12, implementing this solution in the City of Knoxville achieves approximately 179.7 million kg reduction in coal usage, or equivalently, 78.2 million m³ or 107.4 thousand m³ reduction in natural gas or oil usage, respectively. According to EIA (2017b), these values translate into approximately 372 million kg, 152 million kg, and 309 million kg decrease in CO_2 emissions, respectively.

5. Conclusion and Remarks

785

In this study, we evaluate the overall profit from energy generated and saved through installation of PV panels and GRs, while incorporating future climate uncertainties and the interaction between the practices. We study the model over two different planning horizon lengths, T=10 and T=20 years. The results suggest that a 10-year planning horizon is generally too short to allow for a profitable investment. However, a 20-year planning horizon, which is also more consistent with the lifespans of PV panels and GRs, is a better time frame for evaluating the outcomes of an investment on these green technologies. The results also show the importance of incorporating the PV-GR integration efficiency increase as it can significantly change the optimal solutions. The sensitivity analysis demonstrates that different cost and output of PV panels can significantly change the optimal solution. The sensitivity and robustness analyses show that the model is sensitive with respect to GR-

related parameters, suggesting the need for careful calibration of these parameters before large scale implementation in any climate region. Lastly, the results indicate that considering the long-term changes in the rate of energy consumption affects the distribution of budget/rooftop areas between PV panels and GRs.

In this study, we only focus on the energy savings provided by GRs. Future studies may also incorporate other beneficial aspects of utilizing GRs in an urban area (such as run-off reduction, scaling down CO₂ emissions, and heat island mitigation) to more accurately evaluate the overall benefits of installing GRs and their significant role in increasing the urban resiliency. In addition, although the developed model is capable of considering multiple regions, due to limited data availability, especially with regard to future climate projections, in this study we only focus on one region, i.e., Knoxville, Tennessee. Future studies may include using this model to evaluate investment options across multiple regions with different climates.

6. Acknowledgments

The authors thank Jon M. Hathaway and Thom Epps for assisting with data collection and extraction, and providing insights. We also thank the editor and reviewers for their constructive and helpful comments. This work was supported in part by the National Science Foundation Grant CMMI-1634975.

References

- Abdelaziz, F. B., Aouni, B., and El Fayedh, R. (2007). Multi-objective Stochastic Programming for Portfolio Selection. *European Journal of Operational Research*, 177(3):1811–1823.
- Albareda-Sambola, M., Fernández, E., and Saldanha-da Gama, F. (2011). The Facility Location Problem with Bernoulli Demands. *Omega*, 39(3):335–345.
- Alsema, E. A. and Nieuwlaar, E. (2000). Energy Viability of Photovoltaic Systems. *Energy policy* 28(14):999–1010.
- Amato, A. D., Ruth, M., Kirshen, P., and Horwitz, J. (2005). Regional Energy Demand Responses to Climate Change: Methodology and Application to the Commonwealth of Massachusetts. *Climatic Change*, 71(1-2):175–201.

Ampim, P. A., Sloan, J. J., Cabrera, R. I., Harp, D. A., and Jaber, F. H. (2010). Green Roof Growing Substrates: Types, Ingredients, Composition and Properties. *Journal of Environmental Horticulture*, 28(4):244–252.

830

845

- Arnette, A. N. (2013). Integrating Rooftop Solar into a Multi-source Energy Planning Optimization Model.

 Applied energy, 111:456–467.
- Ascione, F., Bianco, N., de'Rossi, F., Turni, G., and Vanoli, G. P. (2013). Green Roofs in European Climates. Are Effective Solutions for the Energy Savings in Air-conditioning? *Applied Energy*, 104:845–859.
- Aurora Energy, a. (2018). Peak Sun Hours. http://www.aurorasolarenergy.com/average-daily-sun-hours/.
 Bankier, C. and Gale, S. (2006). Energy Payback of Roof Mounted Photovoltaic Cells.
 - Banos, R., Manzano-Agugliaro, F., Montoya, F., Gil, C., Alcayde, A., and Gómez, J. (2011). Optimization Methods Applied to Renewable and Sustainable Energy: A Review. Renewable and Sustainable Energy Reviews, 15(4):1753–1766.
- Barbarosolu, G. and Arda, Y. (2004). A Two-stage Stochastic Programming Framework for Transportation Planning in Disaster Response. *Journal of the operational research society*, 55(1):43–53.
 - BCC (2017). Beijing Climate Center, China Meteorological Administration. http://forecast.bcccsm.ncc-cma.net/web/channel-1.htm.
 - Belzer, D. B. (2009). Energy Efficiency Potential in Existing Commercial Buildings: Review of Selected Recent Studies. Technical report, Pacific Northwest National Lab. (PNNL), Richland, WA (United States).
 - Berndtsson, J. C. (2010). Green Roof Performance Towards Management of Runoff Water Quantity and Quality: A Review. *Ecological Engineering*, 36(4):351–360.
 - Bianchini, F. and Hewage, K. (2012). How "Green" are the Green Roofs? lifecycle analysis of green roof materials. *Building and environment*, 48:57–65.
- Birge, J. R. and Louveaux, F. (2011). Introduction to Stochastic Programming. Springer Science & Business Media.
 - Bose, B. K. (2010). Global Warming: Energy, Environmental Pollution, and the Impact of Power Electronics. Industrial Electronics Magazine, IEEE, 4(1):6–17.
- Boston Solar, b. (2018). Solar Panels Lifetime Productivity and Maintenance Costs. http://www.bostonsolar.us/solar-blog-resource-center/blog/solar-panels-lifetime-productivity-and-maintenance-costs/.
 - Burroughs, H. and Hansen, S. J. (2013). Managing Indoor Air Quality Fifth Edition, volume 1. CRC Press.
 - CCSI (2017). Oak Ridge National Laboratory's Climate Change Science Institute. https://ccsi.ornl.gov.
 - Census Bureau, U. S. (2018a). Median and Average Square Feet of Floor Area in New Single-Family Houses Completed by Location. https://www.census.gov/const/C25Ann/sftotalmedaygsqft.pdf.
 - Census Bureau, U. S. (2018b). Number of Stories in New Single-Family Houses Completed. https://www.

census.gov/construction/chars/pdf/stories.pdf.

- Chang, N.-B., Rivera, B. J., and Wanielista, M. (2010). Cost Benefit Optimization of Cistern Volume and Green Roof Area in the Florida Showcase Green Environome (FSGE). In Sustainable Systems and Technology (ISSST), 2010 IEEE International Symposium on, pages 1–6. IEEE.
- Chemisana, D. and Lamnatou, C. (2014). Photovoltaic-green Roofs: An Experimental Evaluation of System Performance. *Applied Energy*, 119:246–256.
- Chen, S.-G. (2013). Bayesian Approach for Optimal PV System Sizing under Climate Change. *Omega*, 41(2):176–185.
- Chow, T. T. (2010). A Review on Photovoltaic/Thermal Hybrid Solar Technology. *Applied energy*, 87(2):365–379.
 - Chung, D., Davidson, C., Fu, R., Ardani, K., and Margolis, R. (2015). US Photovoltaic Prices and Cost Breakdowns: Q1 2015 Benchmarks for Residential, Commercial, and Utility-scale Systems. Technical report, NREL Technical Report, In Preparation.
- ⁸⁷⁵ CMCC (2017). Euro-Mediterranean Center On Climate Change. http://www.cmcc.it/models/cmcc-cm.
 - Coma, J., Pérez, G., Solé, C., Castell, A., and Cabeza, L. F. (2016). Thermal Assessment of Extensive Green Roofs as Passive Tool for Energy Savings in Buildings. *Renewable Energy*, 85:1106–1115.
 - Cook-Patton, S. C. and Bauerle, T. L. (2012). Potential Benefits of Plant Diversity on Vegetated Roofs: A Literature Review. *Journal of Environmental Management*, 106:85–92.
- Correia, I., Nickel, S., and Saldanha-da Gama, F. (2018). A Stochastic Multi-period Capacitated Multiple Allocation Hub Location Problem: Formulation and Inequalities. Omega, 74:122–134.
 - CRONOS (2017). Mc Ghee Tyson Airport (KTYS). http://climate.ncsu.edu/cronos/?station=KTYS.
 - CSIRO (2017). ACCESS Climate Model. http://www.csiro.au/en/Research/OandA/Areas/Assessing-our-climate/CAWCR/ACCESS/.
- ⁸⁵ Current Results Weather and Science Facts (2017). Average Annual Sunshine by State. https://www.currentresults.com/Weather/US/average-annual-state-sunshine.php.
 - Degree Days Weather Data (2017). Custom Degree Day Data. http://www.degreedays.net.
 - Dunec, J. L. (2012). Banking on Green: A look at How Green Infrastructure Can Save Municipalities Money and Provide Economic Benefits Community-Wide.
- EarthClim (2017). Multi-institutional, Coordinated Climate Research in Norway. http://folk.uib.no/ngfhd/ EarthClim/.
 - EIA (2017). Average Price of Electricity to Ultimate Customers by End-use Sector. https://www.eia.gov/electricity/monthly/epm_table_grapher.cfm?t=epmt_5_6_a.
- EIA (2017a). Average Quality of Fossil Fuel Receipts for the Electric Power Industry. https://www.eia. gov/electricity/annual/html/epa_07_03.html.

- EIA (2017b). Carbon Dioxide Uncontrolled Emission Factors. https://www.eia.gov/electricity/annual/html/epa_a_03.html.
- EIA (2017c). Residential Energy Consumption Survey (RECS). https://www.eia.gov/consumption/residential/.
- EIA (2018a). Heating and Cooling No Longer Majority of U.S. Home Energy Use. https://www.eia.gov/todayinenergy/detail.php?id=10271&src=%E2%80%B9%20Consumption%20%20%20%20%20Residential%20Energy%20Consumption%20Survey%20(RECS)-f4.
 - EIA (2018b). Today in Energy. https://www.eia.gov/todayinenergy/detail.php?id=14771

905

910

- EIA, E. (2018c). U.S. Imports of Solar Photovoltaic Modules Mainly Come from Asia. https://www.eia.gov/todayinenergy/detail.php?id=34952.
- EIA, E. I. A. (2015). Annual Energy Outlook 2015 with Projections to 2040. Department of Energy.
- Energy Informative (2017). The Real Lifespan of Solar Panels. http://energyinformative.org/lifespan-solar-panels/.
- Energy Informative, E. (2014). What's the Difference Between Net Metering and Feed-In Tariffs? http://energyinformative.org/net-metering-feed-in-tariffs-difference.
 - Energy Saving Trust, E. (2015). Solar Energy Calculator Sizing Guide. http://www.pvfitcalculator.energysavingtrust.org.uk/Documents/150224_SolarEnergy_Calculator_Sizing_Guide_v1.pdf.
- EPA, E. (2009). Incorporating Low Impact Development into Municipal Stormwater Programs. https://www3.epa.gov/region1/npdes/stormwater/assets/pdfs/IncorporatingLID.pdf.
- EPA, E. (2017). Wind Energy Development in Region 8. https://www.epa.gov/sites/production/files/documents/WindEnergyDevelopmentInReg8Draft19Dec07.pdf.
 - Feed-in Tariffs, f. (2018). What Is the Export Tariff? http://www.fitariffs.co.uk/fits/principles/export/.
 - Feldman, D., Barbose, G., Margolis, R., James, T., Weaver, S., Darghouth, N., Fu, R., Davidson, C., and Wiser, R. (2014). Photovoltaic System Pricing Trends: Historical, Recent, and Near-term Projections. 2014 Edition. *Presentation by SunShot, US Department of Energy, NREL/PR-6A20-62558*.
 - Feng, H. and Hewage, K. (2014). Energy Saving Performance of Green Vegetation on LEED Certified Buildings, Energy and Buildings, 75:281–289.
 - Florida Solar Energy Center, F. (2018). Cell, Modules, and Arrays. http://www.fsec.ucf.edu/en/consumer/solar_electricity/basics/cells_modules_arrays.htm.
- Frischknecht, R., Itten, R., Sinha, P., de Wild-Scholten, M., Zhang, J., Fthenakis, V., Kim, H., Raugei, M., and Stucki, M. (2015). Life Cycle Inventories and Life Cycle Assessment of Photovoltaic Systems.

 International Energy Agency (IEA) PVPS Task, 12(9).
 - Gagnon, P., Margolis, R., Melius, J., Phillips, C., and Elmore, R. (2016). Rooftop Solar Photovoltaic Technical Potential in the United States: A Detailed Assessment. Rep. No. NREL/TP-6A20-65298).

930 Retrieved March, 30:2016.

935

- Gargari, C., Bibbiani, C., Fantozzi, F., and Campiotti, C. A. (2016). Simulation of the Thermal Behaviour of a building retrofitted with a green roof: optimization of energy efficiency with reference to italian climatic zones. *Agriculture and agricultural science procedia*, 8:628–636.
- Gou, B. (2008). Generalized Integer Linear Programming Formulation for Optimal PMU Placement. *IEEE Transactions on Power Systems*, 23(3):1099–1104.
- Green, H. M. and Kozek, A. S. (2003). Modelling Weather Data by Approximate Regression Quantiles. ANZIAM Journal, 44:229–248.
- Green Infrastructure Foundation, g. (2017). Making Informed Decisions: A Green Roof Cost and Benefit Study for Denver. https://static1.squarespace.com/static/588221e420099e47b8fe06d8/t/59e0e8d0017db2106c37d7b5/1507911889792/Denver_Cost_Benefit_Report_Final.pdf.
- Green Roof Technology, g. (2018). Solar Garden Roof First, Fully Integrated Solar and Extensive Green Roof. http://www.greenrooftechnology.com/Solar_PV_Greenroofs.
- Griva, I., Nash, S. G., and Sofer, A. (2009). Linear and Nonlinear Programming. Society for Industrial and Applied Mathematics, Philadelphia.
- GSA, U. (2011). The Benefits and Challenges of Green Roofs on Public and Commercial Buildings. A Report of the United States General Service Administration.
 - GSA, U. G. S. A. (2011). The Benefits and Challenges of Green Roofs on Public and Commercial Buildings. Gurobi, O. (2014). Inc., "Gurobi Optimizer Reference Manual," 2015. *Google Scholar*.
 - Hand, M. M. (2012). Renewable Electricity Futures Study. National Renewable Energy Laboratory.
- Hoffert, M. I., Caldeira, K., Jain, A. K., Haites, E. F., Harvey, L. D., Potter, S. D., Schlesinger, M. E., Schneider, S. H., Watts, R. G., Wigley, T. M., et al. (1998). Energy Implications of Future Stabilization of Atmospheric CO2 Content. *Nature*, 395(6705):881–884.
 - Hong, T., Koo, C., Park, J., and Park, H. S. (2014). A GIS (Geographic Information System)-based Optimization Model for Estimating the Electricity Generation of the Rooftop PV (Photovoltaic) System. *Energy*, 65:190–199.
 - Hostick, D. J., Belzer, D. B., Hadley, S. W., Markel, T., Marnay, C., and Kintner-Meyer, M. C. (2014). Projecting Electricity Demand in 2050. Technical report, Pacific Northwest National Laboratory (PNNL), Richland, WA (United States).
- Huang, Y. (2006). The Impact of Climate Change on the Energy Use of the US Residential and Commercial
 Building Sectors. Lawrence Berkeley National Laboratory, Report No. LBNL-60754.
 - Hui, S. C. and Chan, S. (2011). Integration of Green Roof and Solar Photovoltaic Systems. In *Joint symposium*, pages 1–12.
 - IGRA (2017). International Green Roof Association. http://www.igra-world.com/types_of_green_roofs/.

- IPCC (2017). Intergovermental Panel on Climate Change Data Distribution Centre. http://www.ipcc-data.org/guidelines/pages/gcm_guide.html.
- IPSL (2017). Institut Pierre Simon Laplace Climate Modeling Center. http://icmc.ipsl.fr/.

965

975

- JMA (2017). Japan Meteorological Agency. http://ds.data.jma.go.jp/tcc/tcc/products/gwp/gwp7/html_e/model.html.
- Jun, M., Knutti, R., and Nychka, D. W. (2008). Spatial Analysis to Quantify Numerical Model Bias and
 Dependence: How Many Climate Models Are There? Journal of the American Statistical Association,
 103(483):934–947.
 - Kasper, M., Bortis, D., and Kolar, J. W. (2014). Classification and Comparative Evaluation of PV Panel-integrated DC–DC Converter Concepts. *IEEE Transactions on Power Electronics*, 29(5):2511–2526.
 - Kim, J., Hong, T., and Koo, C.-W. (2012). Economic and Environmental Evaluation Model for Selecting the Optimum Design of Green Roof Systems in Elementary Schools. *Environmental science & technology*, 46(15):8475–8483.
 - Kodysh, J. B., Omitaomu, O. A., Bhaduri, B. L., and Neish, B. S. (2013). Methodology for Estimating Solar Potential on Multiple Building Rooftops for Photovoltaic Systems. Sustainable Cities and Society, 8:31–41.
- Köhler, M., Wiartalla, W., and Feige, R. (2007). Interaction Between PV-Systems and Extensive Green Roofs. In *Proceedings of the Fifth Annual Greening Rooftops for Sustainable Communities Conference, Awards and Trade Show*.
 - Koo, C., Hong, T., Lee, M., and Kim, J. (2016). An Integrated Multi-objective Optimization Model for Determining the Optimal Solution in Implementing the Rooftop Photovoltaic System. Renewable and Sustainable Energy Reviews, 57:822–837.
 - Kornelakis, A. (2010). Multiobjective Particle Swarm Optimization for the Optimal Design of Photovoltaic Grid-connected Systems. *Solar Energy*, 84(12):2022–2033.
 - LASG (2017). Institute of Atmospheric Physics, State Key Laboratory of Numerical Modeling for Atmospheric Sciences and Geophysical Fluid Dynamics. http://www.lasg.ac.cn/.
- Levinson, R., Akbari, H., Pomerantz, M., and Gupta, S. (2009). Solar Access of Residential Rooftops in Four California Cities. *Solar Energy*, 83(12):2120–2135.
 - Li, Y. and Babcock, R. W. (2014). Green Roof Hydrologic Performance and Modeling: A Review. Water Science and Technology, 69(4):727–738.
- Liu, G., Rasul, M., Amanullah, M., and Khan, M. M. K. (2012). Techno-economic Simulation and Optimization of Residential Grid-connected PV System for the Queensland Climate. *Renewable Energy*, 45:146–155
 - Loveland, J. and Brown, G. (1996). Impacts of climate change on the energy performance of buildings in

the united states.

- Mansur, E., Mendelsohn, R., and Morrison, W. (2005). A Discrete-continuous Choice Model of Climate Change Impacts on Energy.
 - Maqsood, I. and Huang, G. H. (2003). A Two-stage Interval-stochastic Programming Model for Waste Management Under Uncertainty. *Journal of the Air & Waste Management Association*, 53(5):540–552.
 - Marmidis, G., Lazarou, S., and Pyrgioti, E. (2008). Optimal Placement of Wind Turbines in a Wind Park Using Monte Carlo Simulation. *Renewable energy*, 33(7):1455–1460.
- Minnesota Stormwater Manual, m. (2018). Cost-benefit Considerations for Green Roofs. https://stormwater.pca.state.mn.us/index.php?title=Cost-benefit_considerations_for_green_roofs.
 - MPI (2017). New Earth System Model Of Max Planck Institute For Meteorology. http://www.mpimet.mpg.de/en/science/models/mpi-esm.html.
 - NCAR (2017). CESM Models. http://www.cesm.ucar.edu/models/ccsm4.0//.
- Niachou, A., Papakonstantinou, K., Santamouris, M., Tsangrassoulis, A., and Mihalakakou, G. (2001).
 Analysis of the Green Roof Thermal Properties and Investigation of Its Energy Performance. Energy and Buildings, 33(7):719–729.
 - Noyan, N. (2012). Risk-averse Two-stage Stochastic Programming with an Application to Disaster Management. Computers & Operations Research, 39(3):541–559.
- Ordóñez, J., Jadraque, E., Alegre, J., and Martínez, G. (2010). Analysis of the Photovoltaic Solar Energy Capacity of Residential Rooftops in Andalusia (Spain). Renewable and Sustainable Energy Reviews, 14(7):2122–2130.
 - Parisio, A. and Jones, C. N. (2015). A Two-stage Stochastic Programming Approach to Employee Scheduling in Retail Outlets with Uncertain Demand. *Omega*, 53:97–103.
- Park, H. S., Jeong, K., Hong, T., Ban, C., Koo, C., and Kim, J. (2016). The Optimal Photovoltaic System Implementation Strategy to Achieve the National Carbon Emissions Reduction Target in 2030: Focused on Educational Facilities. Energy and Buildings, 119:101–110.
 - Porsche, U. and Köhler, M. (2013). Life Cycle Costs of Green Roofs. World Climate & Energy Event.
- Princeton University (2017). Geophysical Fluid Dynamics Laboratory. https://www.gfdl.noaa.gov/ earth-system-model/.
 - Raji, B., Tenpierik, M. J., and van den Dobbelsteen, A. (2015). The Impact of Greening Systems on Building Energy Performance: A Literature Review. Renewable and Sustainable Energy Reviews, 45:610–623.
 - Refahi, A. H. and Talkhabi, H. (2015). Investigating the Effective Factors on the Reduction of Energy Consumption in Residential Buildings with Green Roofs. *Renewable Energy*, 80:595–603.
- Rehman, S., Bader, M. A., and Al-Moallem, S. A. (2007). Cost of Solar Energy Generated Using PV Panels.

 *Renewable and Sustainable Energy Reviews, 11(8):1843–1857.

- Rosenthal, D. H., Gruenspecht, H. K., and Moran, E. A. (1995). Effects of Global Warming on Energy Use for Space Heating and Cooling in the United States. *The Energy Journal*, pages 77–96.
- Ruth, M. and Lin, A.-C. (2006). Regional Energy Demand and Adaptations to Climate Change: Methodology and Application to the State of Maryland, USA. *Energy policy*, 34(17):2820–2833.

- Sailor, D. J. (2001). Relating Residential and Commercial Sector Electricity Loads to Climate—evaluating State Level Sensitivities and Vulnerabilities. *Energy*, 26(7):645–657.
- Sailor, D. J. and Pavlova, A. (2003). Air Conditioning Market Saturation and Long-term Response of Residential Cooling Energy Demand to Climate Change. *Energy*, 28(9):941–951.
- Santamouris, M. (2014). Cooling the Cities–A Review of Reflective and Green Roof Mitigation Technologies to Fight Heat Island and Improve Comfort in Urban Environments. *Solar energy*, 103:682–703.
 - Scherba, A., Sailor, D. J., Rosenstiel, T. N., and Wamser, C. C. (2011). Modeling Impacts of Roof Reflectivity, Integrated Photovoltaic Panels and Green Roof Systems on Sensible Heat Flux into the Urban Environment. *Building and Environment*, 46(12):2542–2551.
- Schneising, O., Reuter, M., Buchwitz, M., Heymann, J., Bovensmann, H., and Burrows, J. (2014). Terrestrial Carbon Sink Observed from Space: Variation of Growth Rates and Seasonal Cycle Amplitudes in Response to Interannual Surface Temperature Variability. *Atmospheric Chemistry and Physics*, 14(1):133–141.
- Scott, M. J., Dirks, J. A., and Cort, K. A. (2005). The Adaptive Value of Energy Efficiency Programs
 in a Warmer World. Technical report, Pacific Northwest National Lab.(PNNL), Richland, WA (United States).
 - SEIA, S. E. I. A. (2018). Net Metering. https://www.seia.org/initiatives/net-metering.
 - Snodgrass, E. C. and Snodgrass, L. L. (2006). Green Roof Plants: A Resource and Planting Guide. Number 04; SB419. 5, S5. Timber Press Portland.
- Solar Direct (2017). Solar Electric System Sizing. http://www.solardirect.com/pv/systems/gts/gts-sizing-sun-hours.html.
 - $Solar\ Power\ Authority, s.\ (2018).\ How\ to\ Calculate\ Your\ Peak\ Sun-Hours.\ https://www.solarpowerauthority.\\ com/how-to-calculate-your-peak-sun-hours/.$
 - Solar Quotes (2017). Inverters. https://www.solarquotes.com.au/inverters/.
- Sonne, J. (2006). Evaluating Green Roof Energy Performance. Ashrae Journal, 48(2):59.
 - Spala, A., Bagiorgas, H., Assimakopoulos, M., Kalavrouziotis, J., Matthopoulos, D., and Mihalakakou, G. (2008). On the Green Roof System. Selection, State of the Art and Energy Potential Investigation of a System Installed in an Office Building in Athens, Greece. *Renewable Energy*, 33(1):173–177.
 - SVS (2017). Renewable Solutions. http://www.svsolar.com/projects/harned.htm.
- The City of Knoxville, C. (2018). 2017-2018 Budget. http://www.knoxvilletn.gov/government/city_

- departments_offices/Finance/budget/budget_archive/2017-2018_budget/.
- Tyagi, V., Rahim, N. A., Rahim, N., Jeyraj, A., and Selvaraj, L. (2013). Progress in Solar PV Technology: Research and Achievement. *Renewable and sustainable energy reviews*, 20:443–461.
- UDI (2017). Oak Ridge National Laboratory's Urban Dynamics Institute. https://udi.ornl.gov.
- Van Hoesen, J. and Letendre, S. (2010). Evaluating Potential Renewable Energy Resources in Poultney, Vermont: A GIS-based Approach to Supporting Rural Community Energy Planning. *Renewable Energy*, 35(9):2114–2122.
 - Van Slyke, R. M. and Wets, R. (1969). L-shaped Linear Programs with Applications to Optimal Control and Stochastic Programming. SIAM Journal on Applied Mathematics, 17(4):638–663.
- Wang, C. and Nehrir, M. H. (2004). Analytical Approaches for Optimal Placement of Distributed Generation Sources in Power Systems. *IEEE Transactions on Power systems*, 19(4):2068–2076.
 - Whaley, C. (2016). Best Practices in Photovoltaic System Operations and Maintenance. Technical report, National Renewable Energy Lab.(NREL), Golden, CO (United States).
 - Wholesale Solar, W. (2018). Power Inverters. https://www.wholesalesolar.com/power-inverters.
- Wiese, S., Libby, L., Energy, A., Long, E., and Ryan, B. (2010). A Solar Rooftop Assessment for Austin. In SOLAR 2010 conference proceedings. Phoenix AZ.
 - Witmer, L. (2010). Quantification of the Passive Cooling of Photovoltaics Using. PhD thesis, The Pennsylvania State University.
 - Witmer, L. and Brownson, J. (2011). An Energy Balance Model of Green Roof Integrated Photovoltaics: A Detailed Energy Balance Including Microclimatic Effects. In *ASES*, pages 17–21.
 - Wong, E., Akbari, H., Bell, R., and Cole, D. (2011). Reducing Urban Heat Islands: Compendium of Strategies. *Environmental Protection Agency, retrieved May*, 12:2011.
 - Yang, C.-J. (2010). Reconsidering Solar Grid Parity. Energy Policy, 38(7):3270-3273.

1085

- Yang, J., Yu, Q., and Gong, P. (2008). Quantifying Air Pollution Removal by Green Roofs in Chicago. Atmospheric environment, 42(31):7266–7273.
- Yongqiang, Y., Xuehong, Z., and Yufu, G. (2004). Global Coupled Ocean-atmosphere General Circulation Models in LASG/IAP. *Advances in Atmospheric sciences*, 21(3):444–455.
- Zhao, M. and Srebric, J. (2012). Assessment of Green Roof Performance for Sustainable Buildings Under Winter Weather Conditions. *Journal of Central South University*, 19(3):639–644.
- Zhou, Z., Zhang, J., Liu, P., Li, Z., Georgiadis, M. C., and Pistikopoulos, E. N. (2013). A Two-stage Stochastic Programming Model for the Optimal Design of Distributed Energy Systems. Applied Energy, 103:135–144.